Budker Institute of Nuclear Physics

M.N.Achasov, M.G.Bek, K.I.Beloborodov, A.V.Berdyugin,
A.V.Bozhenok, A.D.Bukin, D.A.Bukin, S.V.Burdin,
V.V.Danilov, T.V.Dimova, S.I.Dolinsky, V.P.Druzhinin,
M.S.Dubrovin, I.A.Gaponenko, V.B.Golubev, V.N.Ivanchenko,
P.I.Ivanov, I.A.Koop, A.A.Korol, M.S.Korostelev,
S.V.Koshuba, A.P.Lysenko, A.A.Mamutkin, I.N.Nesterenko,
E.V.Pakhtusova, E.A.Perevedentsev, A.A.Polunin, E.G.Pozdeev,
V.I.Ptitsyn, E.E.Pyata, A.A.Salnikov, A.V.Savchkov,
S.I.Serednyakov, V.V.Shary, Yu.M.Shatunov, V.A.Sidorov,
Z.K.Silagadze, A.N.Skrinsky, Yu.V.Usov, A.A.Valishev,
A.V.Varganov, A.V.Vasiljev, Yu.S.Velikzhanin.

First Physical Results from SND Detector at VEPP-2M

BudkerINP 97–78

Novosibirsk
1997

First Physical Results from SND Detector at VEPP-2M

M.N.Achasov, M.G.Bek, K.I.Beloborodov, A.V.Berdyugin,
A.V.Bozhenok, A.D.Bukin, D.A.Bukin, S.V.Burdin,
V.V.Danilov, T.V.Dimova, S.I.Dolinsky, V.P.Druzhinin,
M.S.Dubrovin, I.A.Gaponenko, V.B.Golubev, V.N.Ivanchenko,
P.I.Ivanov, I.A.Koop, A.A.Korol, M.S.Korostelev,
S.V.Koshuba, A.P.Lysenko, A.A.Mamutkin, I.N.Nesterenko,
E.V.Pakhtusova, E.A.Perevedentsev, A.A.Polunin, E.G.Pozdeev,
V.I.Ptitsyn, E.E.Pyata, A.A.Salnikov, A.V.Savchkov,
S.I.Serednyakov, V.V.Shary, Yu.M.Shatunov, V.A.Sidorov,
Z.K.Silagadze, A.N.Skrinsky, Yu.V.Usov, A.A.Valishev,
A.V.Varganov, A.V.Vasiljev, Yu.S.Velikzhanin.

The Budker Institute of Nuclear Physics,
630090, Novosibirsk, Russia

Abstract

The paper describes experiments with the SND detector at VEPP-2M collider, carried out during the period from October 1995 until June 1997. The total integrated luminosity of 6.4 pb^{-1} was collected in the energy range $2E = 0.4 \div 1.4\ GeV$ (MHAD97 experiment), corresponding to $4 \cdot 10^5$ $\mu^+\mu^-$-pairs produced. Preliminary results of the 1996 ϕ-meson experiment (FI96) are presented. The total number of ϕ-mesons produced is $4 \cdot 10^6$. New data on rare decays of ϕ and $\eta(550)$ mesons, in particular

$B(\phi \to \eta\gamma) = (1.30 \pm 0.06 \pm 0.07)$ %,
$B(\phi \to \pi^o\pi^o\gamma) = (1.1 \pm 0.2) \cdot 10^{-4}$, $(M_{\pi^o\pi^o} > 800MeV)$,
$B(\phi \to f^o\gamma) = (4.7 \pm 1.0) \cdot 10^{-4}$,
$B(\phi \to \eta\pi^o\gamma) = (1.3 \pm 0.5) \cdot 10^{-4}$,
$B(\phi \to \eta'\gamma) < 1.7 \cdot 10^{-4}$,
$B(\phi \to 2\pi^o) < 6 \cdot 10^{-4}$

were obtained.

1. The MHAD97 experiment

In the end of 1996 the experiments, started in 1995 with SND detector [2,3], were continued. In the period from October until November the energy range $2E$ from 600 down to 370 MeV was scanned. The total integrated luminosity of 80 nb^{-1} was collected, which corresponds to approximately $3 \cdot 10^4 \mu^+\mu^-$ and $10^4 \pi^+\pi^-$ events. The goal of the experiment was to collect data needed to improve accuracy of calculations of the contribution of this energy region into anomalous magnetic moment of muon. The data were taken in parallel with the CMD–2 [4] detector. The energy dependence of VEPP-2M average luminosity during this experiment is shown in Fig. 1.

In the beginning of January 1997 the VEPP-2M energy was set to approximately $2E = M_\phi$ and data were collected corresponding to integrated luminosity of about 200 nb^{-1} or $0.7 \cdot 10^6$ ϕ-mesons produced.

From the end of January until June 1997, in parallel with the CMD– 2 detector, the MHAD97 experiment in the energy range $2E$ from 980 to 1380 MeV was carried out. Two scans of this energy region were performed: one – upwards, and another – downwards, with a step of $\Delta(2E) = 10$ MeV. The total integrated luminosity collected was 6.3 pb^{-1} at an average luminosity of $1.3 \cdot 10^{30}$ $cm^{-2}s^{-1}$ (Fig. 1), and the total number of recorded events of 10^8, from which about $3.6 \cdot 10^5$ were $\mu^+\mu^-$- pairs, and 10^5 $\pi^+\pi^-$- pairs. In Fig. 2 the weekly schedule of data taking is shown. The mean event recording rate was about ~ 23 Hz and average live time ~ 72 %. The raw events were stored on thirty 8 mm 4 GB tapes.

The main goal of this experiment was a thorough measurement of different hadronic production cross sections, including $e^+e^- \to 2\pi, 3\pi, 4\pi, \omega\pi, K\bar{K}, K\bar{K}\pi, \ldots$. New measurements can facilitate more precise tests of different theoretical models (VDM, CVC, ...), check if there are sizable contributions from radial excitations ρ', ω', ϕ', and determine the contribution of this energy region into muon anomalous magnetic moment.

2. Detector performance

The SND detector was described in detail elsewhere in [1–3]. Simultaneously with data taking the work on improvement of detector parameters was performed. One of the most important parameters is the energy resolution of the calorimeter for electrons and photons. Primary calibration of the calorimeter was done using cosmic muons, and final calibration – using Bhabha events. Recently, progress in understanding of factors limiting the detector resolution (Fig.3) was achieved. It turned out, that nonuniformity of the light collection efficiency in the NaI(Tl) crystals of the inner calorimeter layer contributed significantly into calorimeter response. When this effect was included into simulation program, the disagreement between measured ($\sigma_E/E_\gamma = 5.5\%$ at $E_\gamma = 500$ MeV) and simulated resolution ($\sigma_E/E_\gamma = 4.2\%$) was significantly reduced. The next step in improvement of calorimeter response was implementation of an absolute calibration procedure based on Bhabha scattering events. With such a calibration the energy resolution for electrons and photons was improved by approximately 10%. Such a modest improvement with respect to "cosmic" calibration [5] shows relatively high precision of the cosmic calibration procedure.

Another important parameter of the calorimeter is an invariant mass resolution σ_m/m for particles decaying into photons, which depends on a particle energy and mass. Table 1 shows values of σ_m/m for π^o, η, K_S ω- mesons, extracted from FI96 experimental data [3].

Systematic discrepancy between measured and simulated resolutions, seen in the Ta-

Table 1: Invariant mass resolution (σ_m/m) for particles decaying into photons.

Particle	π^o	η	η	K_S	ω
Energy, MeV	519	657	657	510	801
Process	$\phi \to \pi^o\gamma$	$\phi \to \eta\gamma$	$\phi \to \eta\gamma$	$\phi \to K_S K_L$	$\phi \to \omega\pi^o$
Decay mode	$\pi^o \to \gamma\gamma$	$\eta \to \gamma\gamma$	$\eta \to 3\pi^o$	$K_S \to 2\pi^o$	$\omega \to \pi^o\gamma$
σ_m/m, MC., %	8.1	2.7	2.9	4.4	1.8
σ_m/m, exp., %	10	2.9	3.5	5.2	2.4

ble 1, is still under investigation. For example, in Fig. 4 the ω- meson invariant mass spectrum in the decay channel $\omega \to \pi^o\gamma$ is shown. It was obtained during the study of the process $e^+e^- \to \omega\pi^o \to \pi^o\pi^o\gamma$.

Before the beginning of MHAD97 experiment the performance of the drift chamber system was improved, using for calibration copiously produced collinear e^+e^-- pairs from Bhabha scattering process. The spatial resolution in transverse direction, determined by the accuracy of drift time measurements was equal to 180 microns (σ) on average; the resolution in longitudinal direction was 3.2 mm (σ) for charge division, and 1.5 mm for cathode strip readout. In Fig. 5, 6 the experimental and simulated distributions over $\Delta\varphi$, $\Delta\vartheta$ angles in the Bhabha scattering events are shown. The widths of the distributions are determined not only by spatial resolution of the drift chambers, but also by higher order QED corrections to Bhabha scattering. The intrinsic angular resolution of the drift chambers is $\sigma_\phi = 0.7^o$ in azimuth and $\sigma_\vartheta = 2.2^o$ in polar plane. The performance of drift chambers can also be described in terms of impact parameter ΔR – measured distance between the track of a charged particle and beam axis, projected onto a plane, perpendicular to the beam (Fig. 7). In the infinite spatial resolution limit the average ΔR value must be equal to the transverse size of the beam $\sigma_x = 10$ microns, $\sigma_r = 200$ microns. For the Bhabha scattering events $\sigma_{\Delta R} \simeq 0.4\ mm$ was observed.

The luminosity was monitored during the experiment using the processes of double bremsstrahlung (by an external small-angle monitor), Bhabha scattering, and 2γ-annihilation. Listed below are the selection criteria for events of the two latter processes, used for luminosity monitoring.

For the $e^+e^- \to e^+e^-$ process: number of particles ≤ 4; number of charged particles ≥ 2; distance between tracks and beam collision point $\Delta R \leq 1\ cm$, $\Delta Z \leq 10\ cm$; acollinearity angle $\Delta\varphi \leq 10^o$, $\Delta\vartheta \leq 25^o$; polar angles of both tracks are within $27 \leq \vartheta \leq 153^o$ interval; energy deposition relative to the beam energy $0.6 \leq \Delta E/E \leq 1.5$ for both particles; two-charged-particles trigger must be produced in the event;

For the $e^+e^- \to \gamma\gamma$ **process**: number of particles ≤ 4; number of neutral particles ≥ 2; acollinearity angle between γ- quanta $\Delta\varphi \leq 10^o$, $\Delta\vartheta \leq 25^o$; polar angles of both photons are within $27 \leq \vartheta \leq 153^o$ interval; energy deposition relative to the beam energy $0.6 \leq \Delta E/E \leq 1.5$ for both photons; Two-neutral-particles trigger must be produced in the event.

The luminosity is determined by the following expression for each process: $N_i = L_i\sigma_{oi}$, where i is the fixed beam energy point number; N_i- number of $e^+e^- \to e^+e^-$ or $e^+e^- \to \gamma\gamma$ events; σ_{oi}- detection cross section, calculated with an accuracy up to the third order in α. The ratio of luminosities $L_{\gamma\gamma}/L_{ee}$ for the third scan is shown in Fig. 8. In part of FI96 experiment [3] this ratio was biased from its ideal value by several percent due to low gain in the inner drift chamber.

3. Physical results of FI96 experiment

The FI96 experiment itself was described in our previous preprint [3]. In total, six successive scans were performed ($FI9601 \div FI9606$) with the total integrated luminos-

ity of $\sim 4\ pb^{-1}$, corresponding to approximately 6.5 million ϕ- mesons produced. At present, more than a half of the total recorded data are available for analysis (scans $FI9602 \div FI9604$).

3.1. General description of the SND data analysis

The SND data processing procedure consists of several successive steps [6].

1. Reconstruction of events, stored on primary tapes. For each event a list of particles with their parameters, including energies, angles, etc., is built. Reconstructed events, together with the parameter lists, are written to secondary tapes.

2. Scanning of secondary tapes and creation of third-generation tapes, containing certain event classes, e.g. events containing 6–7 photons, or events with two charged particles and three photons, etc.

3. Events of the classes, mentioned above are downloaded onto hard disks for further processing using well known application packages PAW [7] and MINUIT [8], together with packages, developed in BINP: COCHA data management system [9], GIST histogram code [10], UNIMOD Monte Carlo simulation code [11], ART tape archiving system [12] , and other programs.

The GIST histogram package calculates parameters, specific for the SND. Let us list some of them, the most widely used in data processing:

$E_{tot}/2E$ — total energy deposition in the calorimeter, divided by the center of mass energy $2E$;

$E_{np}/2E$ — sum energy deposition in the calorimeter by neutral particles, measured in the units of the center of mass energy $2E$;

$P_{tot}/2E$ — absolute value of the sum of all particles momenta in an event normalized by a center of mass energy;

N_γ — number of photons, found in an event;

N_{cp} — number of charged particles;

ϑ_i — polar angle of the i-th particle (particles are sorted in the following way: charged particles first, then neutral particles, with descending order in energy within each group);

ϑ_{min} — minimal spatial angle between particles and beam axis;

φ_i — azimuth angle of i-th particle;

R_i — distance between the i-th particle track and beam axis in $R-\varphi$- plane;

Z_i — Z - coordinate of the i-th particle track intersection with beam axis in $R-Z$- plane;

χ^2_E — parameter, characterizing quantitatively the degree to which the energy-momentum conservation law is held in an event, analogous to χ^2 in statistics;

χ^2_m — parameter, characterizing the degree of likelihood of assumption, that there are intermediate π^o or η- mesons in an event;

χ^2_γ — parameter characterizing quality of photons in an event [13], [14].

The total number of parameters available under GIST package is more than 2000. The parameters from this set could be further combined to produce complex constraints and logical formulas for event selection.

During study of processes with substantial statistics the distributions of selected events over beam energy were fitted using the following expression:

$$N_i = L(E_i) \cdot (\sigma(E_i) \cdot \delta(E_i) \cdot \delta_{beam}(E_i) \cdot \varepsilon(E_i) + \sigma_B(E_i)), \qquad (1)$$

where N_i is a number of events in the i-th energy point L — integrated luminosity in this energy point; σ — theoretical cross section of the process under study; δ — factor,

taking into account radiative corrections, calculated for each energy point by convolution of theoretical energy dependence of the cross section with the probability for a photon with a certain energy to be emitted [15]; δ_{beam} — factor, accounting for beam energy spread, also obtained by convolution of radiative corrected cross section with a Gaussian energy distribution of the beam particles; ε — detection efficiency for a process under study for actual event selection criteria, calculated using Monte Carlo simulation; σ_B — total visible cross section for all background processes, calculated in the same way as for the process under study.

Also were taken into account beam energy corrections in individual scans.

The dependence of theoretical cross section on the beam energy for the processes proceeding via intermediate vector resonances $V = \rho,\ \omega,\ \phi$ was approximated as follows (see also [20]):

$$\sigma(E) = |\sum_{i=\rho,\omega,\phi} \sqrt{\sigma_{0V_i}} \cdot \frac{m_{V_i}\Gamma_{V_i}e^{i\delta_{V_i}}}{D_{V_i}(S)}|^2 \qquad (2)$$

.

Here σ_{oV} is a peak cross section; m_V, $\Gamma_V(s)$ are mass and width of the resonance respectively,

$D_V(s) = m_V^2 - s - i\sqrt{s}\Gamma_V(s)$; $s = 4E^2$.

The formulae describing the energy dependence of the resonance widths ($\Gamma_V(s)$) and corresponding references are cited in [20].

To describe the interference between resonant and nonresonant processes the following formula was used:

$$\sigma(E) = \sigma_o(1 + \sigma'(2E - m_\phi)) \cdot |1 - Z\frac{m_\phi\Gamma_\phi}{D_\phi}|^2, \qquad (3)$$

where σ' is a derivative of the nonresonant cross section over energy; Z is a complex amplitude of the resonant process.

3.2. Measurements of ϕ- meson parameters in the process $\phi \to K_SK_L \to neutral\ particles$

The main goal of the study was to obtain the values of m_ϕ, Γ_ϕ, σ_o, and $B(\phi \to K_SK_L)$ with lowest possible statistical error in order to use them in the analyses of other processes with smaller statistics and for evaluation of systematic errors. Given the integrated luminosity of 3.4 pb^{-1} and detection efficiency of $\varepsilon \sim 15\%$, the number of detected $\phi \to K_SK_L \to$ *neutral particles* events could be estimated to be equal to $\sim 10^5$, which leads to a statistical error in a resonance mass: $\sim \Gamma_\phi/2\sqrt{N_\phi} \sim 0.01MeV$. Since the FI96 experiment consisted of six successive scans of the ϕ- region, the study of the K_SK_L production makes possible to check the energy calibration of the collider. Usually the energy scale of the collider depends on many factors. To a relatively good accuracy of better than 20 keV the beam energy can be expressed in the following way: $E(B,T) = k \cdot B + r \cdot T + C$, where B and T are the magnetic field strength and the collider temperature, k, r, C are the parameters to be determined during collider beam energy calibration. The correction accounting for variations of the collider beam circulation frequency $\Delta E/E = -6 \cdot \Delta f/f$ was also included.

Events were selected with $N_\gamma \geq 4$, $0.4 < E_{tot}/2E < 1.2$, with detected $K_S \to 2\pi^o$ decay, and measured m_{K_S} within $400 \div 600MeV$ interval (Fig. 9). Detection efficiency for the $\phi \to K_SK_L$ decay is equal to $\varepsilon = 14.8\%$. For the background $\phi \to \eta\gamma$ process, imitating the process under study due to misidentification of photons, it is equal to $\varepsilon_1 = 1.1\%$. Experimental data were approximated as a sum of the process under study, resonant background from $\phi \to \eta\gamma$, and nonresonant background. The integrated luminosity was

measured using $e^+e^- \to \gamma\gamma$ process. The resonance excitation curve is shown in Fig. 10 and the results of processing of three scans are listed in the Table 2.

Table 2: ϕ- meson parameters from the $e^+e^- \to \phi \to K_S K_L$ process.

	FI9602	FI9603	FI9604	PDG,1996
m_ϕ, MeV	1019.48 ± 0.03	1019.30 ± 0.03	1019.20 ± 0.03	1019.413 ± 0.008
Γ_ϕ, MeV	4.02 ± 0.10	4.59 ± 0.08	4.10 ± 0.08	4.43 ± 0.05
σ_o, nb	1314 ± 17	1322 ± 13	1405 ± 14	1488 ± 22
$B(\phi \to K_S K_L), \%$	30.1 ± 0.4	30.3 ± 0.3	32.2 ± 0.4	34.1 ± 0.5
Number of events	51247	78335	49871	—
χ^2/N_D	10/11	43/12	12/13	—

Main conclusions from the Table 2:

1. There exists a discrepancy between ϕ- meson mass estimations in the second and fourth scans: $\Delta m = 0.28 \pm 0.04 MeV$, which cause is yet unclear.
2. In both 2-nd and 4-th scans χ^2/N_D parameter is small, which is an argument in favor of a good beam energy stability during these scans, at least in the vicinity of the ϕ-meson peak.
3. A beam energy leap presumably occurred in the FI9603 scan. This may explain larger ϕ- meson width and high χ^2/N_D ratio in this scan.
4. Taking into account the former, only FI9602 and FI9604 scans were used for ϕ- meson width determination. The combined result is $\Gamma_\phi = 4.06 \pm 0.08 MeV$. This is by 3 standard deviations smaller than its table value. The corresponding values of decay parameters are the following:

   $\sigma_o = (1360 \pm 11 \pm 45) nb$

   $B(\phi \to K_S K_L) = (31.0 \pm 0.3 \pm 1.0)\%$.

We hope, that processing of the next three scans will clarify situation with systematic errors due to collider energy stability and detector performance.

3.3. Radiative decays

3.3.1. The $\phi \to \eta\gamma$ decay

The $\phi \to \eta\gamma$ decay is a classic magnetic dipole transition from ϕ- into η- meson. In terms of nonrelativistic quark model [19] this decay can be described as a quark spin flip inside ϕ- meson: ${}^3S_1 \to {}^1S_0 + \gamma$. The theoretical estimation and experimental value agree within about 10%. Up to now, more than 10 measurements of $\phi \to \eta\gamma$ branching ratio were done and its current table value is equal to $1.26 \pm 0.06\%$. In this paper preliminary results of new measurements of this parameter in three η- meson decay modes are presented: $\eta \to 2\gamma$ ($B(\eta \to 2\gamma) = 39\%$); $\eta \to \pi^+\pi^-\pi^o$ ($B(\eta \to \pi^+\pi^-\pi^o) = 23\%$) $\eta \to 3\pi^o$ ($B(\eta \to 3\pi^o) = 32\%$).

The $\phi \to \eta\gamma \to 3\gamma$ channel

The following event selection criteria were used: $N_\gamma = 3, 4$; $0.8 < E_{tot}/2E < 1.1$; $P_\perp/2E < 0.175$; $\vartheta_{min} > 24^o$; $E_{\gamma min} > 0.2E$; $550 < m_{\gamma\gamma} < 800 MeV$; $\chi^2_E < 30$. Events from two ϕ- meson scans were processed. Simulated events of the $\phi \to \eta\gamma$; $\phi \to K_S K_L$; $\phi \to \pi^o\gamma$; were processed in the same way in order to evaluate their detection efficiencies, which turned out to be: 22%, 0.01%, and 8% respectively. In Fig. 11 the η- meson invariant mass distribution is shown.

The cross section energy dependence was approximated according to formulae from 1, 2 with a resonant background from the $\phi \to K_S K_L, \pi^o\gamma$ processes and a nonresonant background taken into account. The ϕ- resonance excitation curve in the $\phi \to \eta\gamma$ channel is shown in Fig. 12. The values of fit parameters are listed in Table 3.

Table 3: Main ϕ- meson parameters measured using the $e^+e^- \to \phi \to \eta\gamma \to 3\gamma$ process.

Experiment	FI9602	FI9604	PDG,1996
m_ϕ, MeV	1019.48	1019.2	1019.413 ± 0.008
Γ_ϕ, MeV	4.02	4.1	4.43 ± 0.05
$\sigma_o(e^+e^- \to \phi \to \eta\gamma), nb$	58.9±1.9	59.6±2.2	53.2±2.5
$B(\phi \to \eta\gamma), \%$	1.34±0.05	1.40±0.05	1.26 ± 0.06
Number of events	4256	4040	—
χ^2/N_D	16/10	20/12	—

Combining data from both scans one can obtain the following branching ratio:
$B(\phi \to \eta\gamma) = (1.37 \pm 0.04 \pm 0.08)\%$,
where the first error is a statistical one and the second is systematic.

The $\phi \to \eta\gamma \to 3\pi^o\gamma$ channel

Due to high efficiency of the SND calorimeter to multiphoton events, full reconstruction of $\phi \to \eta\gamma \to 3\pi^o\gamma \to 6,7\gamma$ turned out to be feasible. The characteristic feature of this channel is a peak at η- meson mass in the recoil spectrum of the most energetic photon in an event (Fig. 13). Events were selected according to following criteria: $N_\gamma = 6,7$; $E_{tot}/2E = 0.8 \div 1.2$; $P_{tot}/2E < 0.12$; $\vartheta_{min} > 27^o$, $\chi^2_E < 25$, $\chi^2_\gamma < 20$. For the energy dependence of the cross section the standard approximation was used (2). The energy dependence of the detection efficiency was neglected. The background of ~ 2 % due to the process $\phi \to K_S K_L$ was subtracted using the events outside of the main peak in the Fig. 13.

In order to estimate SND systematic errors for multiphoton events with full reconstruction of all photons, an independent analysis of events with $N_\gamma = 7$ was carried out. In these events the presence of three π^o- mesons was required. The detection efficiency in this case was lower (Table 4), but no background from other ϕ- meson decays was observed at a present level of experimental statistics.

Table 4: Results of the study of $\phi \to \eta\gamma \to \pi^o\pi^o\pi^o\gamma$ decay for three independent scans of the ϕ- resonance region.

	FI9602	FI9603	FI9604
Number of events $6,7\gamma$	1167	1748	1036
$N_{7\gamma}/N_{6\gamma}$ (experiment)	0.60 ± 0.04	0.62 ± 0.04	0.62 ± 0.05
$N_{7\gamma}/N_{6\gamma}$ (simulation)	0.60 ± 0.02	0.60 ± 0.02	0.59 ± 0.02
Number of fully 7γ reconstructed events	360	564	315
Efficiency $6,7\gamma$	8.0 ± 0.1	7.9 ± 0.1	7.7 ± 0.1
Efficiency 7γ	2.72 ± 0.07	2.64 ± 0.07	2.57 ± 0.07
$B(\phi \to \eta\gamma)$ $6,7\gamma$, %	1.24 ± 0.04	1.23 ± 0.03	1.31 ± 0.04
$B(\phi \to \eta\gamma)$ 7γ, %	1.14 ± 0.06	1.17 ± 0.05	1.20 ± 0.07

It is clearly seen from the Table 4 that the cross sections and branching ratios of the process $\phi \to \eta\gamma \to 3\pi^o\gamma$ for the events with $N_\gamma = 6,7$ and $N_\gamma = 7$ differ by approximately 8% (2σ). This systematic error can be explained by misidentification of photons in 7 gamma events.

The data for N_γ =6,7 from all three scans were combined and the following final result was obtained:
$\sigma_o(\phi \to \eta\gamma \to 3\pi^o\gamma) = (54.6 \pm 1.3 \pm 3.5)nb$
$B(\phi \to \eta\gamma) = (1.25 \pm 0.03 \pm 0.08)\%$.

The $\phi \to \eta\gamma \to \pi^+\pi^-\pi^o\gamma$ channel

Since this decay channel in addition to three photons contains two charged particles in its final state, the performance of the drift chambers can contribute into systematic error of the result. Comparison of this result with those for pure neutral channels can be a good probe of the tracking system performance.

Events were selected according to following criteria: $N_{cp} = 2$, $N_\gamma \geq 3$, spatial angle between charged particles $\alpha_{1,2} < 150^o$. Events must satisfy energy and momentum conservation laws with additional requirement, that two photon pairs must have an invariant masses close to that of π^0. This requirement was imposed within a kinematic fitting procedure [16]. This procedure calculated the following parameters: the minimum of logarithmic likelihood function $L_{\eta\gamma}$, m_η — the η- meson mass estimate, D_L — difference between minimums of logarithmic likelihood functions for two best combinations of photons, producing required π^0-s, $D_{L3\pi}$ — difference in likelihood functions minimums in $\eta\gamma$ and $\pi^+\pi^-\pi^o$ hypothesis. In Fig. 14 experimental and simulated distributions over reconstructed mass of the η-meson are shown. After addition of two more requirements: $L_{\eta\gamma} < 15$, $500 < m_\eta < 600MeV$, the detection efficiency was estimated to be $30.4 \pm 0.9\%$, or, taking into account $B(\eta \to \pi^+\pi^-\pi^o) = 0.23$, was equal to $\varepsilon(\eta\gamma \to \pi^+\pi^-\pi^o\gamma) = (7.0 \pm 0.2)\%$

Processing of the FI9602 scan gave the following results on peak cross section and decay branching ratio:

$\sigma_o(e^+e^- \to \phi \to \eta\gamma) = 42.7 \pm 3.1 \pm 4.4nb$

$B(\phi \to \eta\gamma) = (0.98 \pm 0.07 \pm 0.10)\%$.

Only background subtraction error and statistical error of simulation were included into the systematic error.

The data were also processed under more stringent selection criteria: $N_{cp} = 2$, $N_\gamma \geq 3$, $\alpha_{1,2} < 130^o$, $R_{1,2} < 0.5$, $L_{\eta\gamma} < 10$, $D_L > 2$, $D_{L3\pi} < -0.5$, $500 < m_\eta < 600\ MeV$. The detection efficiency here is smaller, $\varepsilon(\eta\gamma \to \pi^+\pi^-\pi^o\gamma) = 5.4 \pm 0.2\%$, but the background was additionally reduced by a factor of 3. Thus, the background subtraction error here was significantly lower.

$\sigma_o(e^+e^- \to \phi \to \eta\gamma) = (48.8 \pm 3.8 \pm 3.8)nb$

$B(\phi \to \eta\gamma) = (1.04 \pm 0.08 \pm 0.08)\%$.

Since the systematic error of the latter result is estimated to be smaller, we consider the last result as a conclusive one for this channel.

Conclusions on the $\phi \to \eta\gamma$ channel

Results obtained for these three different channels do not agree well. Additional study of systematic errors is necessary. Taking into account these differences and common systematic errors, the following combined results can be obtained:

$\sigma_o(e^+e^- \to \phi \to \eta\gamma) = (56.8 \pm 2.6 \pm 3.1)nb$

$B(\phi \to \eta\gamma) = (1.30 \pm 0.06 \pm 0.07)\%$.

3.3.2. The $\phi \to \pi^o\gamma$ decay

The $\phi \to \eta\gamma$ decay was studied on the basis of one scan of ϕ -meson region, corresponding to a total integrated luminosity of $0.4pb^{-1}$ i.e.10% of experimental statistics. The preliminary result was already published in [3] and is equal to

$B(\phi \to \pi^o\gamma) = (0.10 \pm 0.02)\%$.

3.4. Rare radiative decays

3.4.1. Search for the $\phi \to \eta'\gamma$ decay

Radiative decay $\phi \to \eta'\gamma$ is a good probe of an internal structure of the η'- meson [17–19].

As it was mentioned in [17], the $\phi \to \eta'\gamma$ decay branching ratio strongly depends on the gluonium and strange quarks contents in η'- meson. In an assumption of an ordinary quark structure of η', predicted branching ratio is $B(\phi \to \eta'\gamma) = 7 \cdot 10^{-5}$.

Two attempts to measure this decay were done earlier. The first upper limit was obtained with Neutral Detector [20]: $B(\phi \to \eta'\gamma) < 4.1 \cdot 10^{-4}$; and recently was published a preliminary result from CMD-2 detector [21]: $B(\phi \to \eta'\gamma) < 2.4 \cdot 10^{-4}$.

In this work the process

$$\phi \to \eta'\gamma \to \pi^+\pi^-\eta\gamma \to \pi^+\pi^-\pi^+\pi^-\pi^o\gamma \to \pi^+\pi^-\pi^+\pi^-3\gamma \qquad (4)$$

was studied.

Among all decay modes of η'- meson this one has a relatively high probability: $B(\eta' \to \pi^+\pi^-\eta) \cdot B(\eta \to \pi^+\pi^-\pi^o) \sim 10\%$, well defined final state, practically no combinatorial background in neutral particles, and it also contains an η meson in the decay chain.

Event selection for the search of the process (4) was done using the following basic set of conditions: $N_{cp} = 4$; $N_\gamma = 3$; $R_{cp} < 0.3\ cm$; $|Z_{cp}| < 6\ cm$; number of hit wires in the drift chambers corresponds to four tracks. For the events surviving those cuts kinematic fit was performed with additional requirements: $0.1 < E_{np}/2E < 0.3$; energy and momentum conservation is held to the accuracy higher than 10 MeV; minimal spatial angle between any two particles α_{min} is greater than 9 degrees; total energy deposition of charged particles in the second calorimeter layer ΔE_{i2} is less than 40 MeV

In addition, events were required to have some fixed kinematic parameters due to presence of intermediate particles in the decay: recoil mass of one of the photons must be equal to η' mass; invariant mass of the other two photons – equal to π^o mass; and invariant mass of this π^o together with two charged pions – equal to η- meson mass. These masses were calculated for analysis, but no additional cuts were imposed,

Detection efficiency under these selection criteria was determined from simulation to be equal to $\varepsilon = (0.57 \pm 0.07)\%$.

Currently the data from three scans $FI9602 \div FI9604$ were processed, corresponding to a total number of produced ϕ- mesons $N_\phi \sim 4.1 \cdot 10^6$.

Only one event satisfying all intermediate states requirements was found (Fig. 15). Corresponding branching ratio is equal $B(\phi \to \eta'\gamma) = 4 \cdot 10^{-5}$.

The statistics of simulated events of main background processes, available by now, is too low to estimate their contributions and only upper limit corresponding to one detected event could be placed: $B(\phi \to \eta'\gamma) < 1.7 \cdot 10^{-4}$ at 90% confidence level.

3.4.2. Study of electric dipole decays of light vector mesons

Electric dipole transitions are widespread in atoms, but in mesons, composed of light quarks transitions of the type $V \to S\gamma$ ($^3S_1 \to ^3P_o + \gamma$), where V is a vector meson (ρ, ω, ϕ) and S is a scalar one (a_o, f_o, ...) are strongly suppressed by a phase space factor because even the lightest scalar mesons are quite heavy ($M \sim 1\ GeV$).

Quark structure of scalar mesons is not conclusively determined yet. In a standard two-quark description a_o f_o mesons look like scalar analogs of ρ- and ω- mesons:
$a_o = \frac{u\bar{u}-d\bar{d}}{\sqrt{2}}$ and $f_o = \frac{u\bar{u}+d\bar{d}}{\sqrt{2}}$ or $s\bar{s}$.
Better chances has now a four-quark model:
$a_o = \frac{u\bar{u}-d\bar{d}}{\sqrt{2}}s\bar{s}$ and $f_o = \frac{u\bar{u}+d\bar{d}}{\sqrt{2}}s\bar{s}$ [26].
Yet another model was suggested – kaon molecule, according to which, a_o f_o are bound states of two K- mesons ([27], [28]).

And finally, real states can include both ordinary and exotic contributions. The probability of transition $\phi \to S\gamma$ strongly depends on quark structure of mesons involved in the decay. Thus the idea emerged [25] to use radiative decays as a probe in order to

clarify the structure of a_o- f_o- mesons. The results of estimations of branching ratios in different models and the experimental values are listed in Table 5. The most important result is that four-quark model predicts branching ratios almost an order of magnitude higher than two-quark and kaon molecule models.

Table 5: Expected values of scalar meson decays branching ratios from the work [24,25] and experimental results.

	$q\bar{q}$ $(s\bar{s})$	$q\bar{q}q\bar{q}$	$K\bar{K}$	[20]	CMD-2 [21]	This work
$B(\phi \to f_o\gamma \to \pi^o\pi^o\gamma)$	$5 \cdot 10^{-5}$	10^{-4}	10^{-5}	$< 2 \cdot 10^{-3}$	$< 7 \cdot 10^{-4}$	$(4.7 \pm 1.0) \cdot 10^{-4}$
$B(\phi \to a_o\gamma \to \eta\pi^o\gamma)$	$8 \cdot 10^{-6}$	10^{-4}	10^{-5}	$< 2.5 \cdot 10^{-3}$	—	$(1.3 \pm 0.5) \cdot 10^{-4}$

The first time a search for electric dipole transitions was carried out with ND detector [20], where upper limits at a level of $\sim 10^{-3}$ were established. At present the search for the decays of the kind of $\phi \to S\gamma$ is being performed at VEPP-2M collider by two detectors: SND and CMD-2. A new ϕ- factory is close to commissioning in Frascati [29], where the search for such decays was stated as one of the main goals. Another onslaught on neutral decays of ϕ- meson is being prepared at a CEBAF photon beam [30]. So, during next few years one can expect, that situation with these decays will be greatly clarified.

Evidence of the $\phi \to \pi^o\pi^o\gamma$ decay

When studying the

$$e^+e^- \to \phi \to \pi^o\pi^o\gamma \tag{5}$$

channel, one should be aware about significant background contributions, coming from the following processes:

$$e^+e^- \to \phi \to \eta\gamma \to 3\pi^o\gamma, \tag{6}$$

$$e^+e^- \to \omega\pi^o \to \pi^o\pi^o\gamma, \tag{7}$$

$$e^+e^- \to \rho\pi^o \to \pi^o\pi^o\gamma, \tag{8}$$

$$e^+e^- \to \phi \to K_SK_L \to \textit{neutral particles}. \tag{9}$$

Fig. 16 shows expected recoil photons spectra in the processes (5), (7), (8). One can see, that for $E_\gamma < 250\ MeV$ contributions from the processes (7, 8) are significantly suppressed. The processes (6, 9) contribute only due to event misidentification, for example, when photons merge together in the calorimeter. Events were selected satisfying following criteria: $N_\gamma = 5$, $0.8 < E_{tot}/2E < 1.2$, $P_{tot}/2E < 0.12$, $\chi^2_E < 25$. It was also required, that among all combinations of photons existed one, in which two photon pairs have invariant masses within the interval $m_{\pi^o} \pm 30MeV$.

The processes (6, 9) were suppressed with the help of a special parameter, checking if the transverse profiles of photons look like those of isolated ones ($\chi^2_\gamma < 5$). Then, the events with a mass of $\pi^o\gamma$ -system lying within the 720 — 840 MeV interval were discarded in order to reject contribution from the process (7). The $\pi^o\pi^o$ invariant mass spectrum of the remaining events is shown in Fig. 17. Further analysis of the angular distribution revealed, that it agrees with S- wave production mechanism of $\pi^o\pi^o$- system. Detection efficiency for the process (5) under described selection criteria decreases linearly with the increase of $m_{\pi^o\pi^o}$ from 14% at $m_{\pi^o\pi^o} = 800MeV$ to 6% at $975MeV$. This dependence was obtained for the process (5) simulation with two π^o- mesons in S- wave with radiative correction taken into account. The number of events and expected background contributions are listed in the Table 6.

Table 6: Number of the selected events $e^+e^- \to \pi^o\pi^o\gamma$ with $m_{\pi^o\pi^o} > 800MeV$ and estimated background contributions.

N_ϕ	$3.9 \cdot 10^6$
$\phi \to \pi^o\pi^o\gamma$, experiment	45
$\phi \to \eta\gamma$, simulation	5
$\phi \to K_S K_L$, simulation	< 6
$\phi \to \rho\pi^o, \omega\pi^o \to \pi^o\pi^o\gamma$, simulation	1.4
$B(\phi \to \pi^o\pi^o\gamma)$	$(1.1 \pm 0.2) \cdot 10^{-4}$

After background subtraction, in accordance with Table 6, 38 ± 7 events remain, from which the following estimate for the branching ratio could be derived: $B(\phi \to \pi^o\pi^o\gamma) = N_{\pi^o\pi^o\gamma}/N_\phi \cdot \bar{\varepsilon} = (1.1 \pm 0.2) \cdot 10^{-4}$, for $\pi^o\pi^o$- system mass above 800 MeV (only statistical error indicated). So, in this experiment we observe the decay (5) with S- wave production of π^o- pairs. The comparison of $\pi^o\pi^o$ invariant mass spectra, depicted in Fig. 17, with model estimations in Fig. 16 shows good agreement with a four-quark model predictions [25].

Fitting, using formulae of [25], gives the following f_o- meson parameters:
$m_{f_o} = (950 \pm 8)MeV$;
$g^2_{f_oKK}/4\pi = (2.3 \pm 0.5)GeV^{-2}$;
$g^2_{f_o\pi\pi}/4\pi = (0.4 \pm 0.1)GeV^{-2}$;
$B(\phi \to f_o(980)\gamma) = (4.7 \pm 1.0) \cdot 10^{-4}$.

The latter value was obtained within a framework of the 4-quark model ([24,25]). Also taken into account was the relation $B(f_o \to \pi^+\pi^-) = 2B(f_o \to \pi^o\pi^o)$. Systematic error in the branching ratio is estimated to be about 20%. To improve it, one should account for the background from the processes (6, 9) more precisely (look Table 6).

Evidence of the $\phi \to \eta\pi^o\gamma$ decay

The main background for the process

$$e^+e^- \to \eta\pi^o\gamma(\eta \to 2\gamma, \pi^o \to 2\gamma) \to 5\gamma \tag{10}$$

comes from the reactions (6), (7), (9).

The following event selection criteria were used: $N_\gamma = 5$, $\vartheta_{min} > 27^o$, $E_{tot} > 0.8 \cdot 2E_0$, $\chi^2_E < 20$, $\chi^2_M < 25$, $\chi^2_\gamma < 20$, $NC25 < 6$. In the table 7 the corresponding detection efficiencies and number of events are listed. Experimental statistics here is equal to $N_\phi = 6.5 \cdot 10^6$

Table 7: Detection efficiencies and expected number of events for the main processes

	Efficiency	Number of events
Experiment	—	283
$e^+e^- \to \eta\pi\gamma$	$\varepsilon = (8.7 \pm 0.3)\%$	—
$e^+e^- \to \eta\gamma$	$(1.3 \pm 0.1) \cdot 10^{-3}$	109 ± 9
$e^+e^- \to K_S K_L$	$5 \cdot 10^{-6}$	10 ± 10
$e^+e^- \to \omega\pi$	$0.4 \cdot 10^{-2}$	85 ± 4

After background subtraction we obtain the total number of events $N(\phi \to \eta\pi^0\gamma) = 79 \pm 21$, which corresponds to a branching ratio: $B(\eta\pi^0\gamma) = N/N_\phi \cdot \varepsilon = (1.40 \pm 0.35) \cdot 10^{-4}$.

The energy dependence of the visible cross-section was fitted by the sum of process (10), background process $\phi \to \eta\gamma$ and non resonant contribution from the process $e^+e^- \to \omega\pi^0$. The dependence of likelihood function on $B(\phi \to \eta\pi^0\gamma)$ is shown in fig. 18. The optimal value is

$$B(\phi \to \eta\pi^0\gamma) = (1.3 \pm 0.5) \cdot 10^{-4}$$

The mass spectrum of $\eta\pi^o$-system is shown in fig. 19

We also searched for $\phi \to \eta\pi^o\gamma$ decay in $\eta \to \pi^+\pi^-\pi^o$ and $\eta \to 3\pi^o$ decay modes, but due to higher background and lower efficiencies only upper limits for $\phi \to \eta\pi^o\gamma$ branching ratio were obtained:

$B(\phi \to \eta\pi^0\gamma) < 1.5 \cdot 10^{-4}$ $(\eta \to \pi^+\pi^-\pi^0)$,

$B(\phi \to \eta\pi^0\gamma) < 3 \cdot 10^{-4}$ $(\eta \to 3\pi^0)$

at 90% confidence level.

3.4.3. Search for the $\phi \to K_S K_S \gamma$ process

The $\phi \to K_S K_S \gamma$ decay also represents an electric dipole transition, the width of which can be expressed as $M^2\omega^3$, where M is a matrix element and ω is a photon energy. The $K_S K_S$ final state may be produced for example in the decays of light scalar mesons $a_o(980)$ or $f_o(980)$. The expected branching ratio of the $\phi \to K_S K_S \gamma$ decay, obtained on the basis of the theoretical work [25] and table values on $a_o(980)$ $f_o(980)$- mesons [39] , can lie within a wide range of $10^{-7} \div 10^{-9}$. Currently there are no available experimental data on this decay.

The search for $\phi \to K_S K_S \gamma$ decay was performed in the decay mode $\phi \to K_S K_S \gamma \to 2\pi^o 2\pi^o \gamma \to 9\gamma$. The events containing 8 or 9 photons were analyzed with the requirement, that invariant masses of four different photon pairs in an event must be close to a mass of π^o ($m_{\gamma\gamma} = 110 \div 160\ MeV$). Then was required, that of six possible $\pi^o\pi^o$- pairs at least one has an invariant mass close to that of a_o- meson ($430 \div 560\ MeV$). To suppress background from $\phi \to \eta\gamma \to 3\pi^o\gamma \to 7\gamma$ decay, the energy of the most energetic photon in an event was required to be less than 360 MeV. In addition the following constraints were applied: $E_{tot}/2E = 0.8 \div 1.05$; $P_{tot}/2E < 0.2$; $\chi^2_E < 50$.

With such selection criteria the detection efficiency, obtained using simulated events of the process under study, varied from $\varepsilon_1 = 0.4\%$ up to 0.7%, depending on the recoil photon energy $\omega = m_\phi - m_{K_S K_S} = 0 \div 24\ MeV$. The SND threshold for photons is about 10 MeV. The detection efficiency with such a threshold is equal to $(0.7 \pm 0.1)\%$. During processing of experimental data from the scans 2, 3, and 4, total of $N_o = 16$ events were found. All of them could be attributed to a background from $\phi \to K_S K_L$ decay. Thus, the result can be expressed only in terms of an upper limit: $B(\phi \to K_S K_S \gamma) < 2\sqrt{N_o}/N_\phi \varepsilon_1 < 3.2 \cdot 10^{-4}$, at 95% confidence level.

3.5. Rare nonradiative decays of ϕ- meson

3.5.1. The process $e^+e^- \to \omega\pi^o \to \pi^+\pi^-\pi^o\pi^o$

Reaction

$$e^+e^- \to \pi^+\pi^-\pi^o\pi^o \tag{11}$$

was studied in the ϕ- resonance region earlier [20]. This process proceeds purely via $\omega\pi^o$- intermediate state and its cross section is close to 10 nb. The main contribution comes from $\rho(770)$- meson. In the ϕ- peak region the possibility exists to detect contribution from the $\phi \to \omega\pi^o$ decay, which may reveal itself as a narrow interference pattern on a smooth energy dependence of the $\rho(770)$ contribution. Probability of this decay was estimated to be at a level of $5 \cdot 10^{-5}$ [41].

For analysis the events were selected with two charged particles and four photons. The energy-momentum conservation and presence of two π^o- mesons ($\chi^2_M < 30$) were required. To suppress background from the process $e^+e^- \to K^+K^-$, restrictions were imposed on specific ionization losses in the drift chamber. Background from the $\phi \to \eta\gamma \to \pi^+\pi^-\pi^o\gamma$ decay was rejected by a requirement, that the most energetic photon in the event must have an energy less than 360 MeV. The $\phi \to \pi^+\pi^-\pi^o$ decay can also fake the process under study if some stray photons are detected. To suppress it, an additional requirement was

imposed: if the invariant mass of the two most energetic photons is close to that of π^o-meson, then invariant mass of the other pair must differ from it.

Event detection efficiency under these selection criteria, estimated using simulation, is equal to $\varepsilon = 20\%$. In the recoil mass spectrum of π^o- mesons, shown in Fig. 20, the ω-meson peak is clearly seen. On the other hand, presence of a nonresonant contribution is an evidence of some background with intermediate states other than $\omega\pi^o$. To account for this background the special subtraction procedure was developed. It is based on background estimation in the kinematic regions not containing the process under study.

The energy dependence of the cross section was approximated according to the formula (3), with Z, the complex interference amplitude, varying, according to theory, in the limits: $Z = [(11 \div 34) - i(11 \div 24)] \cdot 10^{-2}$, and decay probability, described by an expression:

$B(\phi \to \omega\pi^o) = \sigma_o(m_\phi)|Z|^2/\sigma_\phi$.

For approximation the detection cross section was expressed as in (1), and the result of the procedure is shown in Fig. 21. The following values of parameters were obtained:

$\sigma_o = 6.4 \pm 0.5 \pm 1.0\ nb$ – reaction (11) cross section via $\omega\pi^o$- intermediate state,

$ReZ = (10 \pm 7) \cdot 10^{-2}$; $ImZ = (0 \pm 6) \cdot 10^{-2}$; $\chi^2/N_D = 7/9$.

Systematic error of $\sim 15\%$ is caused by inexact simulation and background subtraction error. As could be seen from Fig. 21 and the values presented above, it is possible to establish only the following upper limit of the decay branching ratio:

$B(\phi \to \omega\pi^o) < 5 \cdot 10^{-5}$ at 90% confidence level.

The contribution of non- $\omega\pi^o$ intermediate states is a subject of further investigation.

3.5.2. The $e^+e^- \to \mu^+\mu^-$ process near ϕ- resonance

Measurements of lepton widths of light vector mesons ρ, ω, ϕ at electron-positron colliders were usually performed through summation of cross sections over all decay channels. Study of the process

$$e^+e^- \to \mu^+\mu^- \tag{12}$$

in the vicinity of the ϕ- peak gives the possibility of direct measurement of $B_{\mu\mu} \equiv B(\phi \to \mu^+\mu^-)$. Expected value of $B_{\mu\mu}$, calculated from $\mu - e$- universality, is equal to:

$$B_{\mu\mu} \simeq B_{ee} = (3.00 \pm 0.06) \cdot 10^{-4} \tag{13}$$

The world average value, taken from PDG (1996) [39]:
$B_{\mu\mu} = (2.48 \pm 0.34) \cdot 10^{-4}$.

The cross section of the process (12) in the vicinity of the ϕ- resonance can be expressed (in linear approximation) in the form (3), where $Z = 3\sqrt{B_{\mu\mu}B_{ee}}e^{i\beta}/\alpha$, and β is an interference phase.

Events were selected according to following conditions: $N_{cp} = 2$; $N_\gamma = 0$; $\Delta\vartheta < 20^o$; $\Delta\varphi < 10^o$; $|Z_{1,2}| < 8\ cm$; $R < 1\ cm$; $\vartheta_{min} > 45^o$.

The main sources of background were the following:

1) $e^+e^- \to e^+e^-$, was rejected using e/π- separation;

2) $e^+e^- \to \pi^+\pi^-$, was suppressed using the outer anticoincidence system of the detector.

3) cosmic muons. These events are not peaked in time, measured by outer scintillation counters, with respect to a beam crossing. On the contrary, the events of the process (1) are strongly peaked with a RMS of $\sigma \sim 1ns$. This permits to reject main part of cosmic muons. Remaining background is suppressed by limiting maximum distance from charged particle tracks to the beam axis.

The detection efficiency for the process (1) is described by the following formula:

$\varepsilon_{\mu\mu} = \varepsilon_{sel} \cdot \varepsilon_\vartheta \cdot \varepsilon_{up} \cdot \varepsilon_\mu \cdot \varepsilon_{FLT} \simeq 0.32$,

where $\varepsilon_{sel} = 0.75$ is a detection efficiency in the conditions, listed above;

$\varepsilon_\vartheta = 0.55$ is an acceptance in polar plane;

$\varepsilon_{up} = 0.99$ is the efficiency of anticoincidence counters;

$\varepsilon_\mu = 0.82$ probability for a muon to trigger outer system;

$\varepsilon_{FLT} = 0.97$ in the second scan, and 0.91 in the third and fourth scans — first level trigger efficiency.

At first, fit was performed with an interference phase as a free parameter. The result was $\beta = 0.13 \pm 0.11$. Then the value of β was set to zero and the fit was repeated. The results are shown in Fig. 22 and in Table 8.

Table 8: The results of cross section fitting for the $e^+e^- \to \mu^+\mu^- process$

Experiment name	σ_o,nb	σ', $10^{-2} MeV^{-1}$	$B_{\mu\mu}$, 10^{-4}	χ^2/N_D
FI9602	96.7±1.6	-0.05±0.21	2.8±1.4	9.2/6
FI9604	95.9±1.2	0.13±0.12	2.2±0.9	12.2/9
FI9602&FI9603&FI9604	96.7±0.9	0.09±0.09	2.4±0.8	29/26

The errors indicated in the Table 8 are all statistical. Possible sources of additional systematic errors are contributions from other decays of ϕ- meson (for example: $\phi \to K^+K^-, \rho\pi, ...$); systematic errors in simulation, inadequate treatment of radiative corrections. In this preliminary analysis the systematic error in σ_o was estimated to be about 5% and the error in $B_{\mu\mu}$ — 20%. Let us finally list the main results:

$\sigma_o = 96.8 \pm 0.9 \pm 5.0\ nb$,

$B_{\mu\mu} = (2.4 \pm 0.8 \pm 0.6) \cdot 10^{-4}$,

$B_{e\mu} = \sqrt{B_{ee} \cdot B_{\mu\mu}} = (2.74 \pm 0.44 \pm 0.6) \cdot 10^{-4}$.

3.6. Rare decays of $\eta(550)$- meson

3.6.1. Upper limit of the $\eta \to 2\pi^o$ decay

CP-violation is one of the most intriguing puzzles in the particle physics. Up to now the only place, when CP-violation was observed was a neutral kaons system. Standard Model (SM) predicts much more pronounced effects in decays of B- mesons.

Flavor conserving CP- violating effects, like $\eta \to 2\pi$ decay, within a framework of SM are very weak: $B(\eta \to \pi^+\pi^-) < 2 \cdot 10^{-27}$ [31,32]. But some other, different from SM, models exist in which such effects are many orders of magnitude larger. $B(\eta \to \pi^+\pi^-) < 10^{-15} \div 10^{-16}$ [32–34]. In any case, search for such unusual effects can produce interesting and unexpected results.

The only existing experimental upper limit — $B(\eta \to \pi^+\pi^-) < 1.5 \cdot 10^{-3}$ was reported in the work [35]. Recently this result was confirmed by CMD-2 detector: $B(\eta \to \pi^+\pi^-) < 2 \cdot 10^{-3}$[21]. In this work search for the process $\eta \to \pi^o\pi^o$, with η-s produced in the reaction $e^+e^- \to \phi \to \eta\gamma$ was carried out.

Events for analysis were selected with two π^o- mesons and a photon, satisfying energy–momentum conservation. The estimated detection efficiency is equal to 8.6%. In Fig. 23 photon recoil mass spectra in the process $e^+e^- \to \phi \to \eta\gamma \to \pi^o\pi^o\gamma$ are shown. Fig. 23a depicts an expected spectrum in the process being searched for; Figs. 23b,c show spectra for the main background processes, and Fig. 23d — experimental data. Unfortunately the number of simulated events is not yet sufficient to determine contribution from $\phi \to K_S K_L$ (statistics at least equal to the experimental one is needed, i.e. $\sim 4 \cdot 10^6$ ϕ- mesons). As it is seen in Fig 23d, there is no indication of the $\eta \to \pi^o\pi^o$ decay and thus, only upper limit can be placed:

$B(\eta \to \pi^o\pi^o) < 6 \cdot 10^{-4}$ at 90% confidence level.

3.7.1. The $e^+e^- \to 3\gamma$ reaction

This process is interesting from the point of view of QED testing near ϕ- resonance and as an important source of background in the studies of the decays $\phi \to \eta\gamma, \pi^o\gamma \to 3\gamma$.

Events were selected according to following criteria: $N_\gamma = 3$; $\vartheta_{min} > 27^o$; $0.75 < E_{tot}/2E < 1.1$; $P_{tot}/2E < 0.1$; $\chi^2_\gamma < 15$; $\chi^2_E < 30$.

The Dalitz plot for the selected events is shown in Fig. 24. Regions of ϕ- meson decays $\phi \to \eta\gamma, \pi^o\gamma \to 3\gamma$, are marked and events from them were excluded from further analysis. The energy dependence of the visible cross section for the selected events is shown in Fig. 25. The estimated cross section at 510 MeV is equal to $\sigma_{MC} = 2.03 \pm 0.07\ nb$, while the experimental value is 20% smaller: $\sigma_{exprm} = 1.56 \pm 0.16 \pm 0.20\ nb$. The cause of such discrepancy is under study. In Fig. 26 the spectrum of the least energetic photon in an event is presented. One can see, that the largest difference between theory and experiment lies in the region $E_{min}/E \sim 0.5$.

The $e^+e^- \to 3\gamma$ process is a source of background for neutral decays of vector mesons and, on the other hand, its cross section is precisely known. Its investigation is important for understanding of systematic errors in other neutral processes and accuracy of luminosity estimations.

3.7.2. The process $e^+e^- \to e^+e^-\gamma$ and search for $\eta \to e^+e^-$ decay

The process $e^+e^- \to e^+e^-\gamma$ is important for us due to several reasons:

1. this process can be used for testing of QED and should be taken into account as a correction for Bhabha scattering, in order to achieve accuracy of luminosity measurements of $\leq 1\%$.

2. this process is a background to different hadronic processes, i.g. $\phi \to \pi^o\gamma, \eta\gamma \to e^+e^-\gamma$.

This process was studied earlier in several experiments: with OLYA detector [36] with an integrated luminosity of $\Delta L = 1.5\ pb^{-1}$, at ADONE collider [37] with $\Delta L = 0.12\ pb^{-1}$.

The results of this work are based on data corresponding to integrated luminosity of $1.8\ pb^{-1}$. During data processing the subset of events with Dalitz pairs was also included. In such events the invariant mass of e^+e^-- pair is very small and the whole process looks like a two-photon annihilation in which one of photons is slightly out of a mass shell, and it subsequently decays into e^+e^-- pair.

The $e^+e^-\gamma$ final state is favorable for the search of the decay $e^+e^- \to \phi \to \eta\gamma \to e^+e^-\gamma$. The $\eta \to e^+e^-$ decay is strongly suppressed in comparison with $\eta \to \gamma\gamma$ by a helicity factor $(m_e/m_\eta)^2$ and additional QED suppression factor α^2. As a result the expected branching ratio is about $5 \cdot 10^{-9}$ [38]. The similar decay $\pi^o \to e^+e^-$ was observed at a level of $\sim 10^{-7}$. Current upper limit of the $\eta \to e^+e^-$ is equal to $2 \cdot 10^{-4}$ [40]

Event selection was done using the following main criteria: $N_{cp} = 2$; $N_\gamma = 1, 2$; $\vartheta_{min} > 36^o$; $R < 0.5cm$; $|Z| < 10cm$; $E_{tot}/2E > 0.8$; $P_{tot}/2E < 0.15$; $\Delta\varphi_{ee} > 5^o$; $\chi^2_E < 40$; $\Delta\Omega_{ee} < 50^o$ — spatial angle between particles for Dalitz pairs.

Fig. 27 shows the photon energy spectrum and in Fig. 28 the distribution over angle between electrons is shown. There is also a region indicated, where the angle between electrons is very small (Dalitz pairs). The number of events in this region is in agreement with an expected one.

Energy dependence of the $e^+e^- \to e^+e^-\gamma$ cross section was approximated using the following expression:

$\sigma_{vis}(E) = \varepsilon_1 \sigma_o(\frac{2E}{E})^2 + \varepsilon\sigma_{3\pi}$.

The first term is responsible for the process under study, while the second describes background from decays of ϕ- meson, especially $\phi \to 3\pi$. It was estimated from background simulation, that $\varepsilon = (0.10 \pm 0.03)\%$. The ε_1 coefficient was determined as a ratio between the number of simulated events, satisfying selection criteria and the total number of simulated events. The simulation was conducted with the following constraints: $\vartheta_{min} > 27^o$, $E_\gamma > 5\ MeV$, and corresponding total cross section under such constraints is equal to $\sigma_o = 570 \pm 15\ nb$, and ε_1 was found to be equal to $(3.5 \pm 0.1)\%$;

The following results were obtained for approximation parameters: $\sigma_o = 550 \pm 10\ nb$; $\varepsilon = (0.08 \pm 0.05)\%$; $\chi^2/N_D = 10/11$. Only statistical errors are indicated. Additional systematic error is estimated as 10%.

The $\eta \to e^+e^-$ decay could reveal itself as a peak in the photon spectrum in Fig. 27 at $E_\gamma = 360\ MeV$. The detection efficiency, obtained from simulation is $\varepsilon_2 = (40 \pm 1)\%$. After fitting of the spectrum the following upper limit was obtained: $B(\eta \to e^+e^-) < 9 \cdot 10^{-4}$. Although this limit is higher than that of PDG Table, increase in statistics and taking into account the energy dependence of the spectrum shape will permit us to improve this result.

3.7.3. $e^+e^- \to \omega\pi^o \to \pi^o\pi^o\gamma$

There are several reasons of interest to the $e^+e^- \to \omega\pi^o$ process. First, in this process may manifest themselves radial excitations of ρ- meson. Second, this process contributes into the total cross section of e^+e^-- annihilation into hadrons. Third, its cross section is connected with the branching ratio of τ- lepton decay into $\omega\pi\nu_\tau$.

Within the Vector Dominance Model (VDM) cross section of this process is determined by $g_{\rho\omega\pi}$ constant, which also controls other processes: $\omega \to 3\pi, \pi^o\gamma$; $\rho \to \pi^o\gamma$; $\pi^o \to 2\gamma$, etc.

In our case the possibility arises to measure this constant at $\sqrt{s} = 1\ GeV$, which can help to determine boundaries of applicability of simple VDM model.

The process $e^+e^- \to \omega\pi^o$ in the energy region $2E > 1\ GeV$ was studied earlier in the experiments with ND detector at VEPP-2M in two main decay modes of ω- meson: $\omega \to \pi^o\gamma$ [42] and $\omega \to \pi^+\pi^-\pi^o$ [20,43].

Some indirect results on this reaction were extracted from τ- lepton decay spectra [20,44].

In this paper data on the process $e^+e^- \to \omega\pi^o \to \pi^o\pi^o\gamma$ in the energy range $2E = 1000 \div 1034\ MeV$ are presented. Results are based on experimental statistics from FI96 SND experiment corresponding to integrated luminosity of $1.9\ pb^{-1}$ or 4 million ϕ- mesons produced.

The main event selection criteria are: $N_\gamma = 5$, $E_{tot}/2E = 0.75 \div 1.25$, $\vartheta_{min} > 27^o$, $P_{tot}/2E < 0.1$.

Then additional requirements were imposed: $\chi^2_M < 40$; $\chi^2_\gamma < 20$; two photon pairs with $m_{\gamma\gamma} = m_{\pi^o} \pm 30\ MeV$ which could be produced by intermediate π^o- mesons must be found in the event; $720 < m_{\pi^o\gamma} < 840\ MeV$.

Selected events originate mainly from the process under study: $e^+e^- \to \omega\pi^o \to \pi^o\pi^o\gamma$. However they contain some background from the decay $\phi \to \eta\gamma \to 3\pi^o\gamma$. The detection efficiency was estimated by simulation. For the process under study it is equal to $\varepsilon_1 = 21\%$ and for the background — $\varepsilon_2 = (1.8 \pm 0.1) \cdot 10^{-3}$. As for another background source: $\phi \to K_S K_L \to$ *neutral particles*, the available simulation statistics is not sufficient to estimate its contribution (minimum 10^6 events are required, while only $6 \cdot 10^4$ are currently available).

In Fig. 4 the distributions over invariant mass of $\pi^o\gamma$- system in experimental and simulated events are shown. It is clearly seen that most of events contain intermediate ω- meson. In Fig. 4 of two possible $\pi^o\gamma$- pairs in an event only one with the mass closest to that of ω- meson is histogrammed. The number of experimental events in the ω- peak region is equal to 304, while expected background from the decay $\phi \to \eta\gamma$ is 92 events. The background from $\phi \to K_S K_L$, according to available simulation statistics, is not more than 20 events. This background could be further suppressed by additional constraint on invariant mass of $\pi^o\pi^o$- system to exclude the $K_S \to 2\pi^o$ decay region.

The energy dependence of the $e^+e^- \to \omega\pi^o$ cross section was approximated using parameterization (3) with $B(\omega \to \pi^o\gamma) = 8.5 \pm 0.5\%$, and taking into account contributions of background processes $\phi \to K_S K_L, \eta\gamma$ into $\sigma_B(E_i)$. In this approximation due to small statistics the contribution from $\phi \to \rho\pi, \omega\pi^o \to \pi^o\pi^o\gamma$ was neglected and thus the energy dependence of the cross section was described by a simple linear function. As a result of fitting of the visible cross section (Fig. 29) the following results were obtained:

$\sigma_o(m_\phi) = 7.5 \pm 1.5 \pm 0.5\ nb$ — the cross section of $e^+e^- \to \omega\pi^o \to \pi^o\pi^o\gamma$ in the ϕ-meson peak (previous ND'1991 result ([20])was $\sigma_o(m_\phi) = 8.7 \pm 1.0 \pm 0.7\ nb$); $\sigma'(m_\phi) = 9 \pm 6\ MeV^{-1}$ — relative slope of the cross section at the same energy; $P(\chi^2) = 12.3/9$.

The $g_{\rho\omega\pi}$ value in an assumption of ρ-meson dominance is equal to:

$g_{\rho\omega\pi}(experimental) = 18.1 \pm 1.7\ GeV^{-1}$.

in VDM this constant equals to:

$g_{\rho\omega\pi}(estimated) = 14.3\ GeV^{-1}$.

In the ND experiment [20,42] the cross section was larger, but it does not contradict the new SND result. The SND data confirm conclusion of the ND experiment that pure $\rho(770)$ production cannot describe the data and to take into account production of higher resonances ρ', ω', ϕ' is necessary.

3.7.4. Production of Δ- barion

When electron beam travels through the collider beam pipe the following process may occur on nuclei of residual gas atoms: $e^\pm A \to e^\pm\Delta \to e^\pm N\pi$ [45]. The $\Delta(1232)$ is a barion state with quantum numbers: $I(J^P) = \frac{3}{2}(\frac{3}{2}^+)$. At a beam energy of $E = 510\ MeV$ the total cross section of this process $\sim 3\mu b$. $\Delta(1232)$ decays into the following final states: $\Delta^+ \to p\pi^o, n\pi^+$ $\Delta^o \to p\pi^-, n\pi^o$.

An attempt was taken to observe this process with SND detector and to study it as a possible source of background at future ϕ- factories.

The process was studied in the:

$$e^\pm p \to e^\pm\Delta^+ \to e^\pm p\pi^o \tag{14}$$

channel because it has a distinct signature: two photons from π^o- meson decay, slow proton track with high dE/dx in the drift chamber, another track of $e^\pm$, zero total transverse momentum and large longitudinal momentum – $P = 510\ MeV/c$.

The events with $N_{cp} = 2$, $N_\gamma = 2$, $E_{tot}/2E < 0.5$, $|Z| < 10\ cm$, etc. were selected. Then kinematic fit was performed.

As a result of experimental events processing in the energy region of ϕ- peak with integrated luminosity of $\Delta L = 0.5\ pb^{-1}$, 36 events were found. Photons in these events have an invariant mass coinciding with that of π^o- meson within $\pm 15\ MeV$. These events are uniformly distributed in Z- coordinate within $\pm 10\ cm$ from the interaction point and show no peaking there. Among two charged particles, one with lower specific ionization was referred to as an electron and another – as a proton. In Fig. 30 the specific ionization in the drift chamber as a function of particle momentum is shown for particles after kinematic fit for experimental and simulated events. One can see, that protons are well

separated from electrons. The Δ- barion mass spectrum in Fig. 31 shows good agreement between experiment and simulation.

The background from ϕ- meson decays is still questionable because of insufficient simulation statistics, but it is obviously not high. It can be seen from absence of peaking of the events near the beam interaction point.

Detection efficiency was estimated from the simulation and was found to be $\varepsilon = 2\%$. Given the pressure of residual gas of about $3 \cdot 10^{-9} Torr$, mean beam current of 15 mA, duration of the experiment $7 \cdot 10^5$ s, and taking into account residual gas composition of $50\% - H_2$, $30\% - CO$, $20\% - CO_2$ [45], one should expect $N \sim 4000$ events of Δ-barion electroproduction at $20cm$ interaction region length. Taking into account the detection efficiency, the number of observed events is expected to be equal to 30 (14). It agrees well with $N_o = 36$ events detected in experiment. We should mention, that there is a considerable uncertainty in the pressure and chemical composition of residual gas. Presence of CO_2, N_2, etc. may lead to a considerable increase in events number.

In conclusion, we can say, that event rate of this process $\sim 6 \cdot 10^{-3}$ s^{-1} is too small to affect other processes under study, but at future ϕ- factories it should be taken into account (14) as a possible source of background.

4. Recent results

In August 1997 just before printing of this preprint the following new upper limits for processes with multiphoton final states were obtained:

- $B(\phi \to 2\pi^0) < 4 \cdot 10^{-5}$
- $B(\phi \to \eta\pi^0) < 5 \cdot 10^{-5}$
- $B(\phi \to 3\pi^0) < 0.8 \cdot 10^{-5}$

The event selection criteria were similar to those applied in the studies of the processes described above, like $\phi \to \eta\gamma \to 3\pi^0\gamma$ or $\phi \to \eta\pi^0\gamma$.

Also was performed search for $K_S \to 3\pi^0$ decay. The event selection criteria were adjusted for $\phi \to K_S K_L$ events with $K_S \to 3\pi^0$ decay and with completely undetected K_L. No indications of $K_S \to 3\pi^0$ decay were found and the upper limit $B(K_S \to 3\pi^0) < 1.1 \cdot 10^{-4}$ was placed.

5. Conclusions

The SND detector continues data taking at VEPP–2M collider. In 1997 the MHAD97 experiment in the energy range $2E$ from 980 up to 1380 MeV and total integrated luminosity of 6.3 pb^{-1} was carried out. The work is under way on improvement of energy and spatial resolution of the detector. About 50% of experimental statistics of the FI96 experiment, collected in 1996 in the energy range $2E = 984 \div 1040\ MeV$ were analyzed. New preliminary results on ϕ- η- mesons decays were obtained (Table 9).

Cross sections of the following nonresonant processes were measured in this energy region:

$\sigma_o(e^+e^- \to \omega\pi^o(\omega \to \pi^+\pi^-\pi^o)) = 6.4 \pm 0.5 \pm 1.0\ nb$;
$\sigma_o(e^+e^- \to \omega\pi^o(\omega \to \pi^o\gamma)) = 7.5 \pm 1.5 \pm 0.5\ nb$;
$\sigma_o(e^+e^- \to \mu^+\mu^-) = 96.8 \pm 0.9 \pm 5.0\ nb$;
$\sigma_o(e^+e^- \to \gamma\gamma\gamma) = 1.56 \pm 0.16 \pm 0.20\ nb$, at $\vartheta_{min} > 27^o$;
$\sigma_o(e^+e^- \to e^+e^-\gamma) = 550 \pm 10 \pm 55nb$, at $\vartheta_{min} > 27^o$ $E_\gamma > 5\ MeV$.

Electroproduction of Δ- barion on residual gas nuclei was seen: $e^\pm A \to e^\pm\Delta \to e^\pm N\pi$.

Table 9: SND preliminary results on $\phi(1020), \eta(550), K_S$ decays, compared with CMD-2 [21], [22], [23] results and data from PDG [39].

Decay mode	SND	CMD-2	PDG(1996)
$\phi \to \eta\gamma$	$(1.30 \pm 0.06 \pm 0.07)\%$	$(1.25 \pm 0.10)\%$	$(1.26 \pm 0.06)\%$
$\eta \to \gamma\gamma$	$(1.37 \pm 0.04 \pm 0.08)\%$		
$\eta \to 3\pi^0$	$(1.25 \pm 0.03 \pm 0.08)\%$		
$\eta \to \pi^+\pi^-\pi^0$	$(1.04 \pm 0.08 \pm 0.08)\%$		
$\phi \to \pi^0\gamma$	$(0.13 \pm 0.005 \pm 0.008)\%$	—	$(0.131 \pm 0.013)\%$
$\phi \to \eta'(958)\gamma$	$< 1.7 \cdot 10^{-4}$	$< 2 \cdot 10^{-4}$	$< 4.1 \cdot 10^{-4}$
$\phi \to K_S K_S \gamma$	$< 3.2 \cdot 10^{-4}$	—	—
$\phi \to \pi^0\pi^0\gamma$	$(1.1 \pm 0.2) \cdot 10^{-4}$	—	$< 1 \cdot 10^{-3}$
$\phi \to \pi^+\pi^-\gamma$	—	$< 1.5 \cdot 10^{-5}$	$< 7 \cdot 10^{-3}$
$\phi \to \mu^+\mu^-\gamma$	—	$(2.3 \pm 1.0) \cdot 10^{-5}$	—
$\phi \to \eta\pi^0\gamma$	$(1.3 \pm 0.5) \cdot 10^{-4}$	—	$< 2.5 \cdot 10^{-3}$
$\phi \to f_0\gamma$	$(4.7 \pm 1.0) \cdot 10^{-4}$	$< 1 - 7 \cdot 10^{-4}$	$< 2 \cdot 10^{-3}$
$\phi \to \rho\gamma$	—	$< 3 \cdot 10^{-4}$	$< 7 \cdot 10^{-2}$
$\phi \to K_S K_L$	0.31 ± 0.02	0.325 ± 0.010	0.341 ± 0.005
$K_S \to 3\pi^0$	$< 1.1 \cdot 10^{-4}$	—	$< 3.7 \cdot 10^{-5}$
$\phi \to \mu^+\mu^-$	$(2.4 \pm 1.0) \cdot 10^{-4}$	—	$(2.48 \pm 0.34) \cdot 10^{-4}$
$\phi \to e^+e^-$	—	$(2.84 \pm 0.06) \cdot 10^{-4}$	$(3.00 \pm 0.06) \cdot 10^{-4}$
$\phi \to \eta e^+e^-$	—	$(1.1 \pm 0.5) \cdot 10^{-4}$	$(1.3^{+0.8}_{-0.6}) \cdot 10^{-4}$
$\phi \to \pi^0 e^+e^-$	—	$(1.1 \pm 0.8) \cdot 10^{-5}$	$< 1.2 \cdot 10^{-4}$
$\phi \to \omega\pi$ $(\pi^+\pi^-\pi^0\pi^0)$	$< 7 \cdot 10^{-5}$	—	—
$\phi \to \pi^+\pi^-\pi^+\pi^-$	—	$< 3 \cdot 10^{-5}$	$< 8.7 \cdot 10^{-4}$
$\phi \to 2\pi^0$	$< 4 \cdot 10^{-5}$	—	—
$\phi \to 3\pi^0$	$< 0.8 \cdot 10^{-5}$	—	—
$\phi \to \eta\pi^0$	$< 7 \cdot 10^{-5}$	—	—
$\eta \to e^+e^-$	$< 9 \cdot 10^{-4}$	—	$< 3 \cdot 10^{-4}$
$\eta \to \pi^0\pi^0$	$< 7 \cdot 10^{-4}$	—	—
$\eta \to \pi^+\pi^-$	—	$< 9 \cdot 10^{-4}$	$< 1.5 \cdot 10^{-3}$

References

[1] V.M.Aulchenko et al., Proc. Workshop on Physics and Detectors for DAΦNE, Frascati, April 9 – 12, 1991. Ed.G.Pancheri, INFN, FRASCATI, 1991, p.605.

[2] V.M.Aulchenko et al., Proc. of HADRON'95, the 6th International Conference on Hadron Spectroscopy, the University of Manchester, Manchester UK, 10 – 14 July, 1995, p.295

[3] M.N.Achasov et al., Preprint, Budker INP 96-47, Novosibirsk, 1996.

[4] E.V.Anashkin et al., ICFA Instrumentation bulletin 5 (1988) 18.

[5] M.N.Achasov et al., Nucl. Instr. and Meth. A379 (1996) 505.

[6] D.A.Bukin et al., Proc. of the International conference on Computing in High Energy Physics, Berlin, April 7-11, 1997.

[7] R.Brun et al., PAW Physics Analysis Workstation CERN Computer Center Program Library.

[8] F.James, M.Roos, MINUIT CERN Computer Center Program Library.

[9] V.N. Ivanchenko, Preprint INP 94-25, Novosibirsk, 1994;
K.Hanssgen, V.N.Ivanchenko, Proceedings of the International conference on Computing in High Energy Physics, Berlin, April 7-11, 1997.

[10] A.D. Bukin, V.N. Ivanchenko, Preprint 93-84, Novosibirsk, 1993.

[11] A.D.Bukin et al., Preprint BudkerINP 94-20, Novosibirsk, 1994.

[12] A.A.Korol, Preprint INP 94-62, Novosibirsk, 1994;
A.D.Bukin et al., Proc. of the International conference on Computing in High Energy Physics, Berlin, April 7-11, 1997

[13] M.G.Bekishev, V.N.Ivanchenko, Nucl. Inst. and Meth. A361 (1995) 138.

[14] A.V.Bozhenok, V.N.Ivanchenko, Z.K.Silagadze, Nucl. Inst. and Meth. A379 (1996) 507.

[15] J.P. Berge et al., Rev. Scien. Instr. 32 (1961) 538.

[16] A.D.Bukin, Preprint Budker INP 97 – 50, Novosibirsk, 1997;
A.D.Bukin, Report at CHEP–97 (Computing in High Energy Physics), April 7 – 11, Berlin, 1997.

[17] J.L.Rosner, Phys. Rev. D (1983) 1101.

[18] F.J.Gilman, R.Kauffman, Phys. Rev.D (1987) 2761.

[19] P.J.O'Donnell, Rev. of Mod. Phys., (1981) 673.

[20] S.I.Dolinsky et al., Phys. Rep. orts 202 (1991) 99.

[21] R.R.Akhmetshin et al., Proc. of the 28-th International Conference on High Energy Physics, Warsaw, Poland, 25 – -31 July 1996 522.

[22] R.R.Akhmetshin et al., Proc. of the 28-th International Conference on High Energy Physics, Warsaw, Poland, 25 – -31 July 1996 1207.

[23] R.R.Akhmetshin et al., Phys. Lett. B 364 (1995) 199.

[24] N.N.Achasov, V.V.Gubin, Phys. Rev. D 56 (1997) 4084.,
hep-ph/9703367

[25] N.N.Achasov, V.N.Ivanchenko, Nucl.Phys. B315 (1989) 465.

[26] N.N.Achasov, S.A.Devyanin, G.N.Shestakov, Usp.Phys.Nauk. 142 (1984) 361.

[27] F.E.Close, N.Isgur, S.Kumano, Nucl.Phys. B389 (1993) 513.

[28] J.Weinstein, N.Isgur, Phys.Rev. D27 (1983) 588.

[29] N.Broun and F.E.Close, The second DAΦNE Physics Handbook, Vol.2, Ed. L.Maiani et al., Frascati. Italy (May 1995), p.649.

[30] A.R.Dzierba, Second Workshop on physics and detectors for DAΦNE, Frascati, April 4 – 7, 1995, Ed. R.Baldini et al., INFN, Frascati, 1995, p.99.

[31] C.Jarlskog and E.Shabalin, Phys. Rev. D52 (1995) 248.

[32] C.Jarlskog and E.Shabalin, Phys. Rev. D52 (1995) 6327.

[33] R.J.Crewther et al., Phys. Lett. 88B (1979) 123.

[34] M.A.Shifman, A.I.Vainstein, V.I.Zakharov, Nucl. Phys. B166 (1980) 494.

[35] J.J.Thaler, J.A.Appel, A.Kotlewski et al., Phys. Rev. D7 (1973) 2569.

[36] A.D.Bukin et al., Preprint BINP 81-109, 1981, Novosibirsk.

[37] C.Bacci et al., Phys. Lett. 71B (1977) 227.

[38] M.J.Savage, M.Luke, M.B.Wise, Phys. Lett. 291B (1992) 481.

[39] Review of Particle Physics, Phys.Rev. D Vol.54 (1996)

[40] D.B.White et al., Phys. Rev. 53D (1996) 6658.

[41] N.N.Achasov, A.A.Kozhevnikov. Intern. Journal of Mod.Phys. 7 (1992) 4825.

[42] S.I.Dolinsky et al., Phys. Lett. 174 (1986) 453.

[43] V.M.Aulchenko et al., Preprint INP 87 – 90, Novosibirsk, 1987;
V.M.Aulchenko et al., Preprint INP 86 – 106, Novosibirsk, 1986.

[44] N.Albrecht et al., Phys. Lett. B185 (1987) 223.

[45] M.N.Achasov et al., Zh. ETP Letters, 65 (1997) 259.

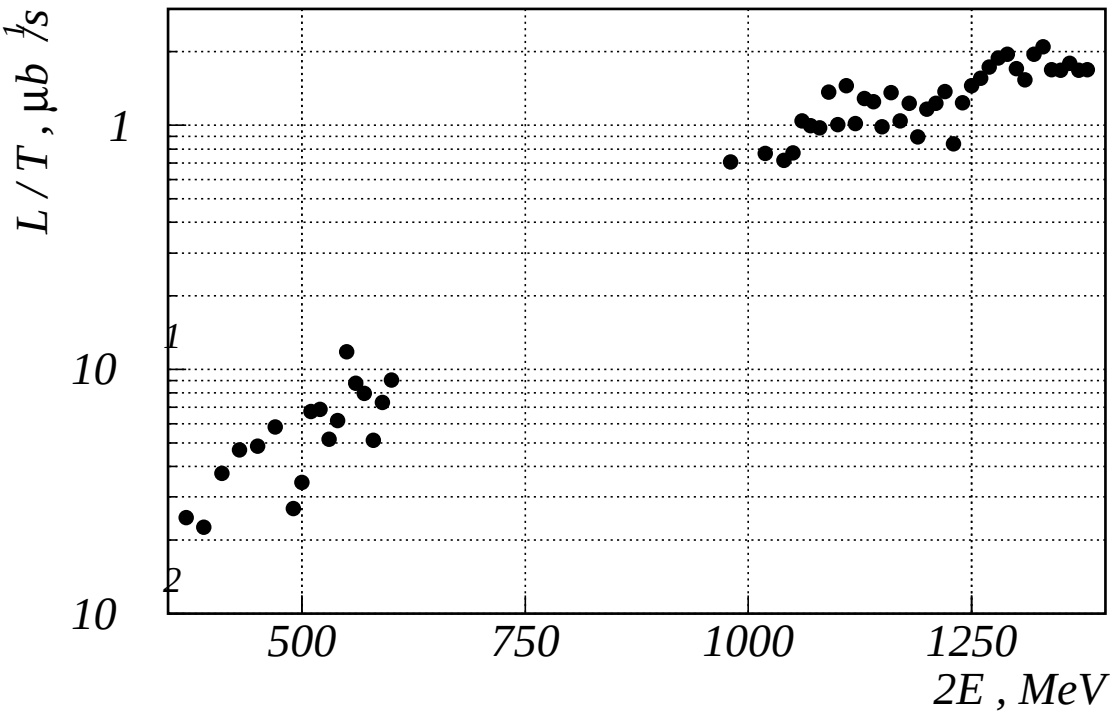

Figure 1: Average luminosity (integrated luminosity at each energy point divided by corresponding live time of data taking) in the experiments with SND detector as a function of the beam energy.

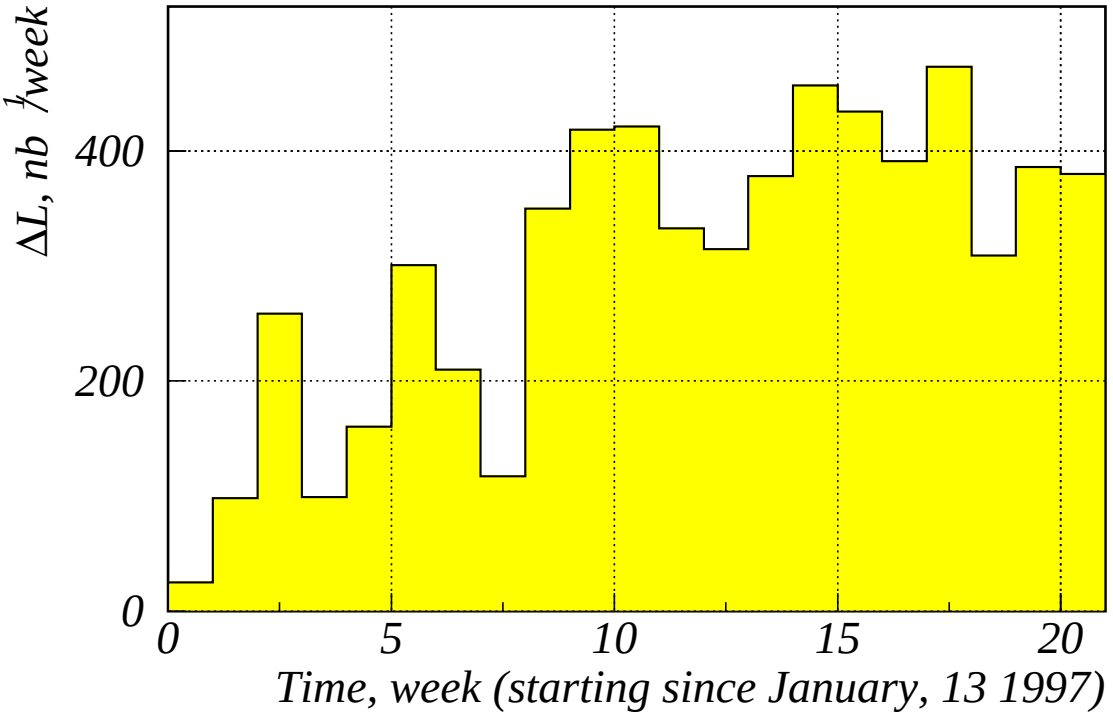

Figure 2: SND total integrated luminosity accumulation schedule in the period from 01/13/1997 to 06/13/1997.

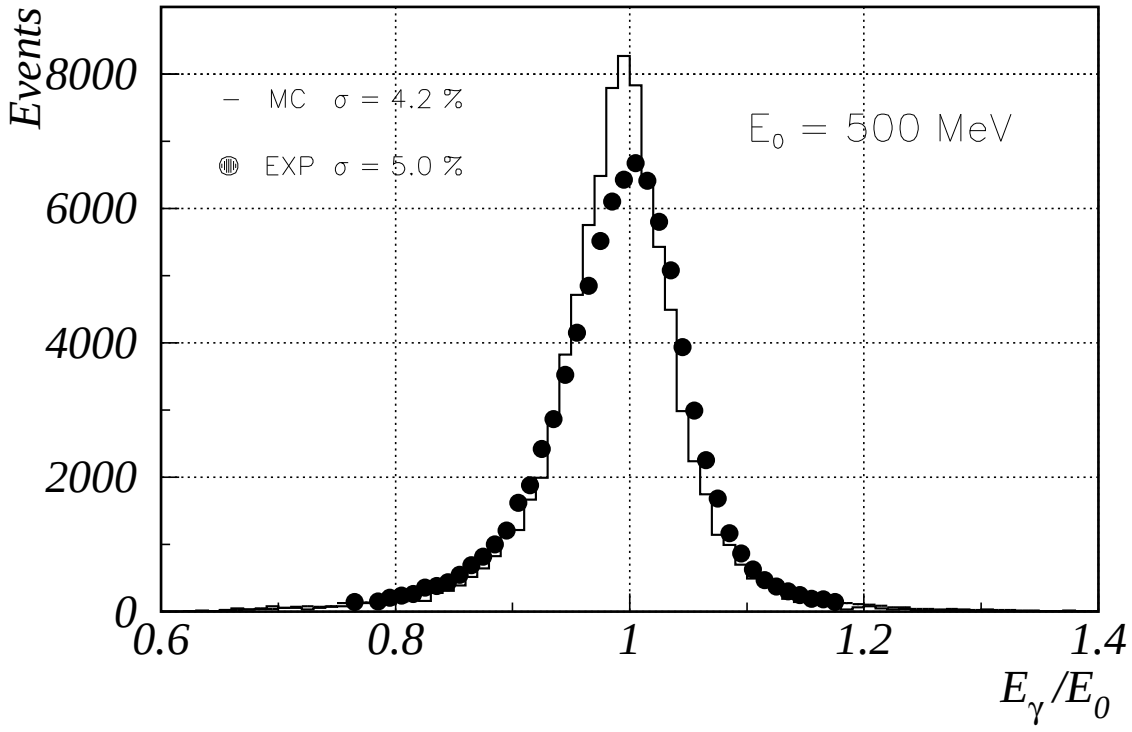

Figure 3: Distribution of $e^+e^- \to \gamma\gamma$ events over normalized energy deposition in the calorimeter. Points — experimental data, $\sigma_{exp.} = 5.0\%$; histogram — simulation, $\sigma_{M.C.} = 4.2\%$.

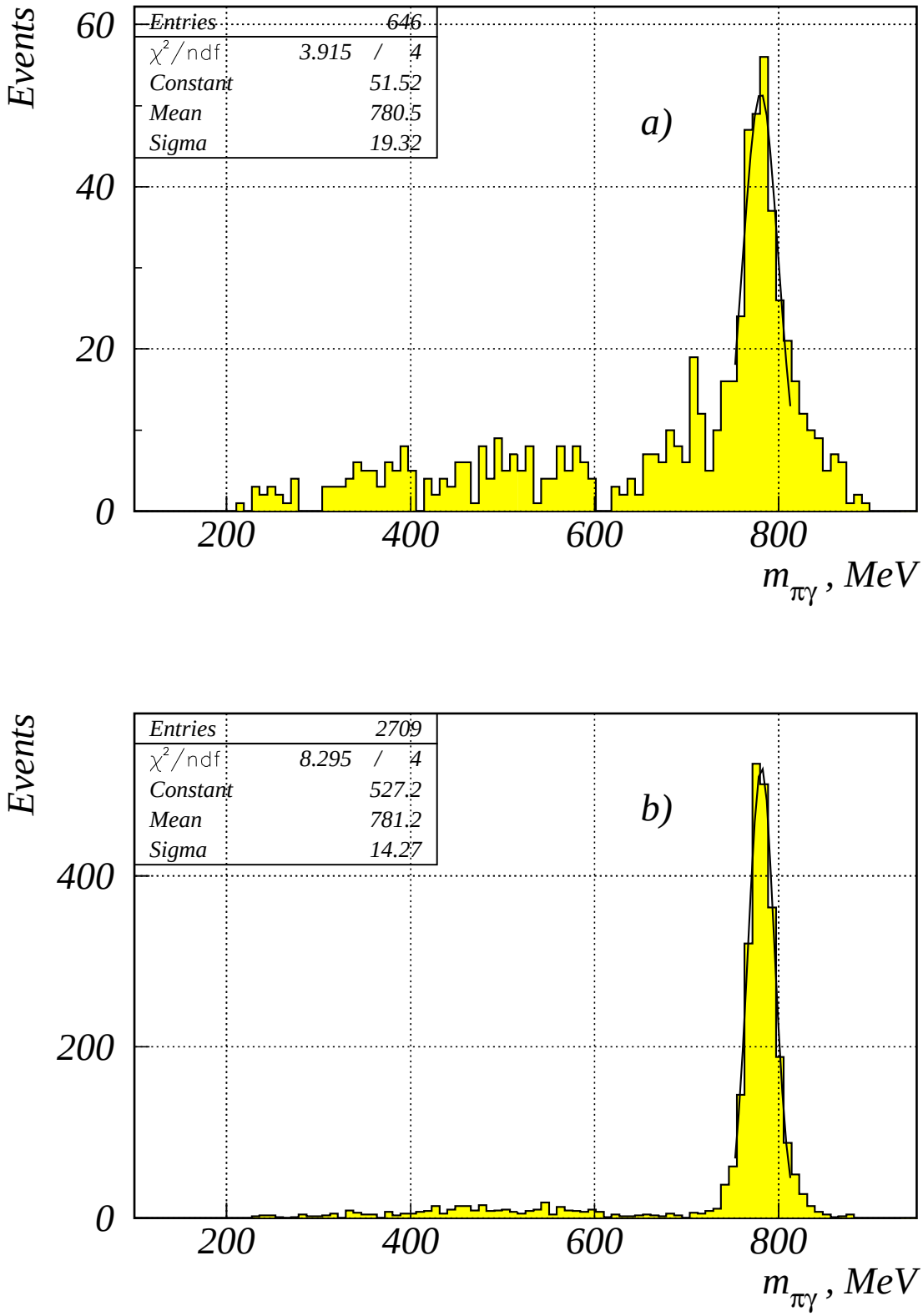

Figure 4: Distribution of the events over $\pi^o\gamma$ invariant mass in the $e^+e^- \to \omega\pi^o \to \pi^o\pi^o\gamma$ process; a — experiment, b — simulation.

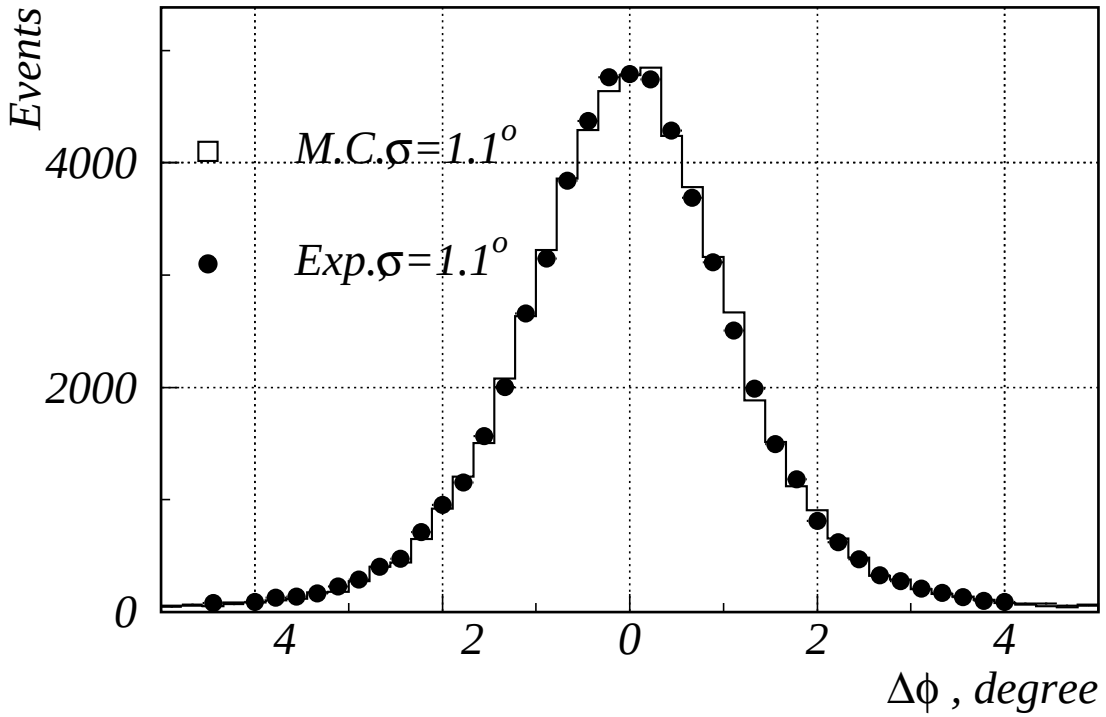

Figure 5: Acollinearity angle distribution in azimuth plane in the $e^+e^- \to e^+e^-$ events.

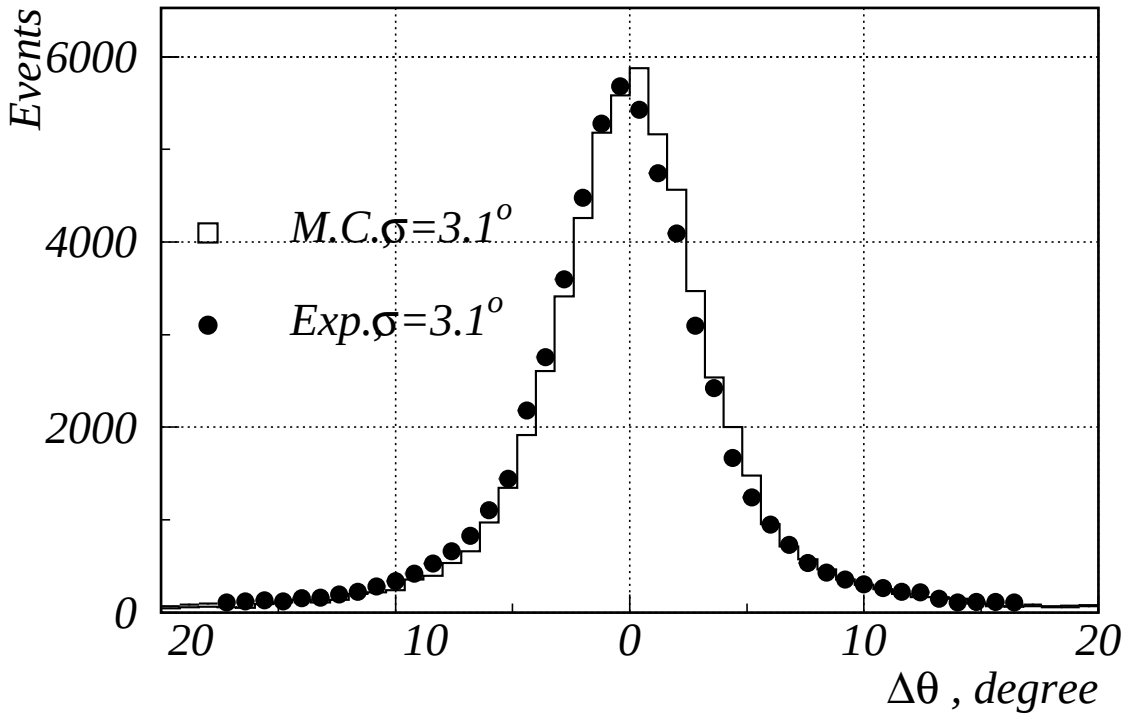

Figure 6: Polar acollinearity angle distribution in the $e^+e^- \to e^+e^-$ events.

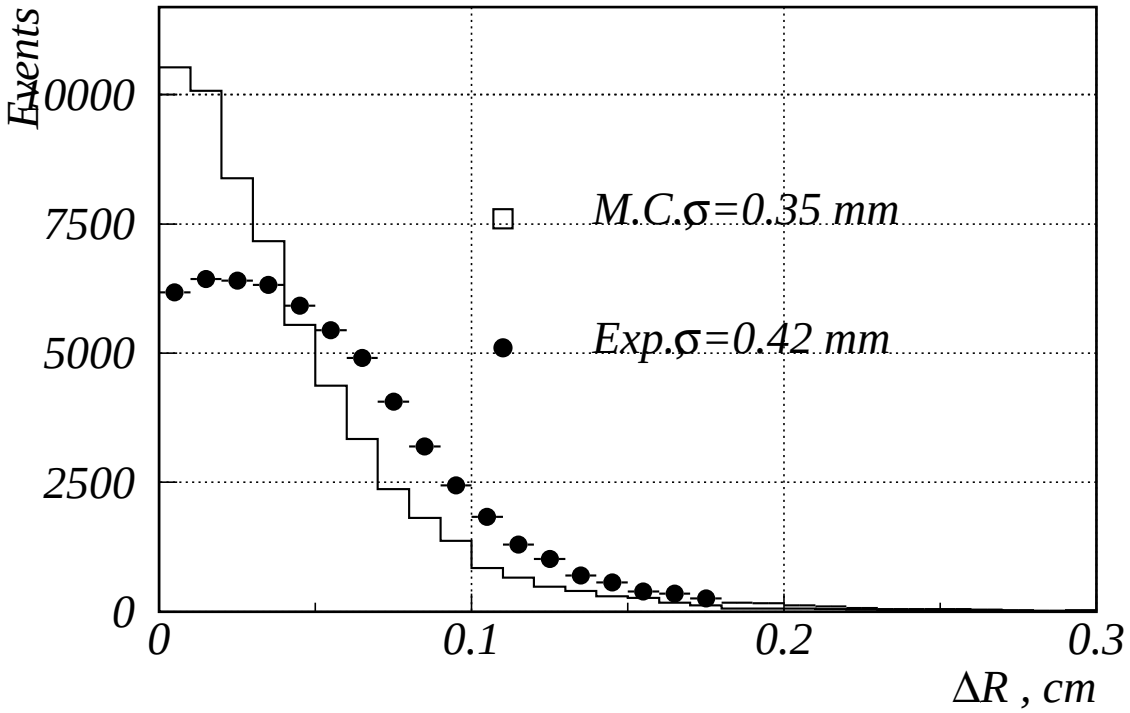

Figure 7: Distribution over the distance from a track to the beam axis ΔR in the $e^+e^- \to e^+e^-$ events.

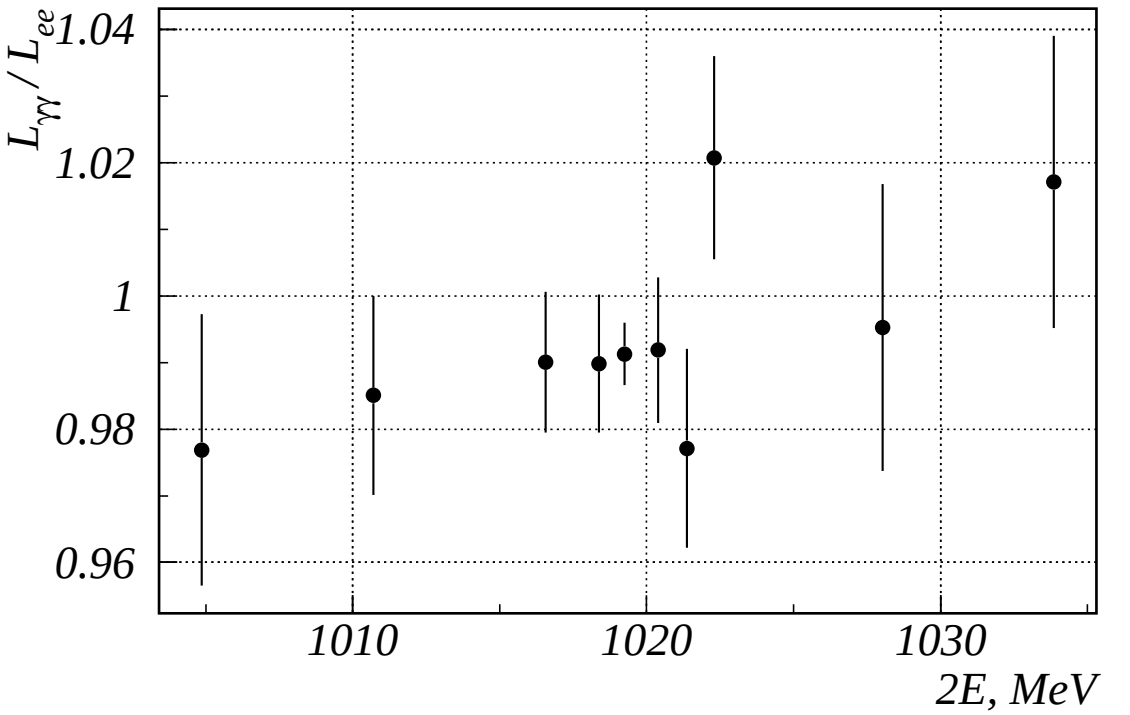

Figure 8: Ratio of the luminosities $L_{\gamma\gamma}/L_{ee}$ in the FI9602 scan [3].

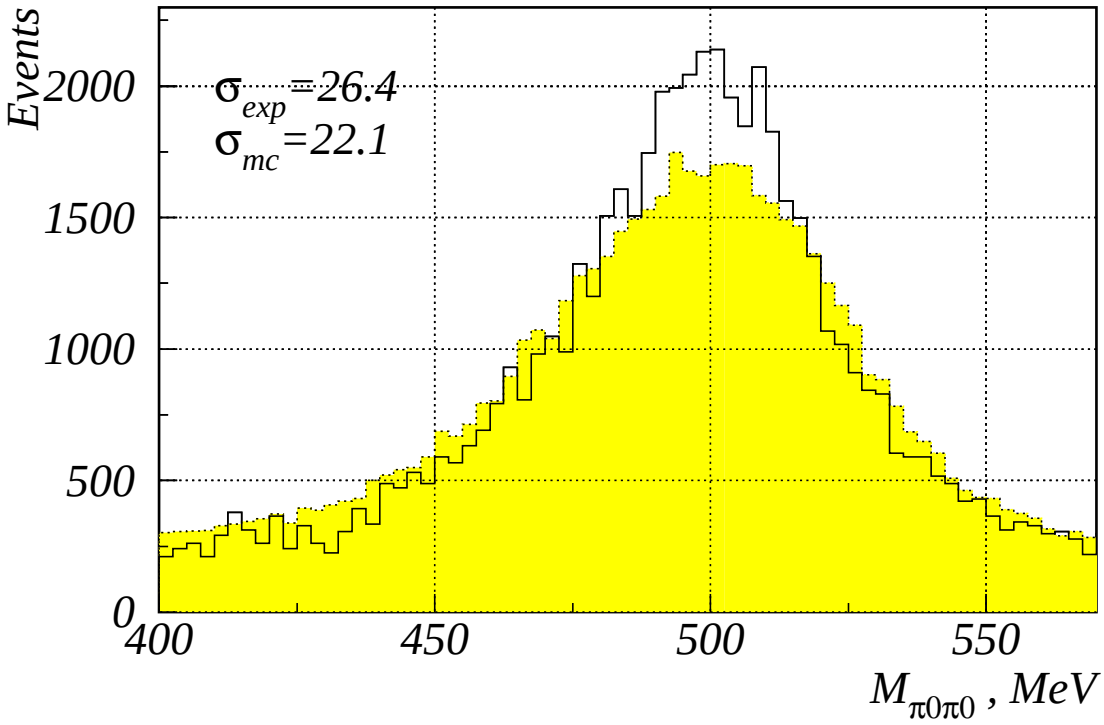

Figure 9: Invariant mass distribution of π^o- meson pairs from the $K_S \to 2\pi^o$ decays.

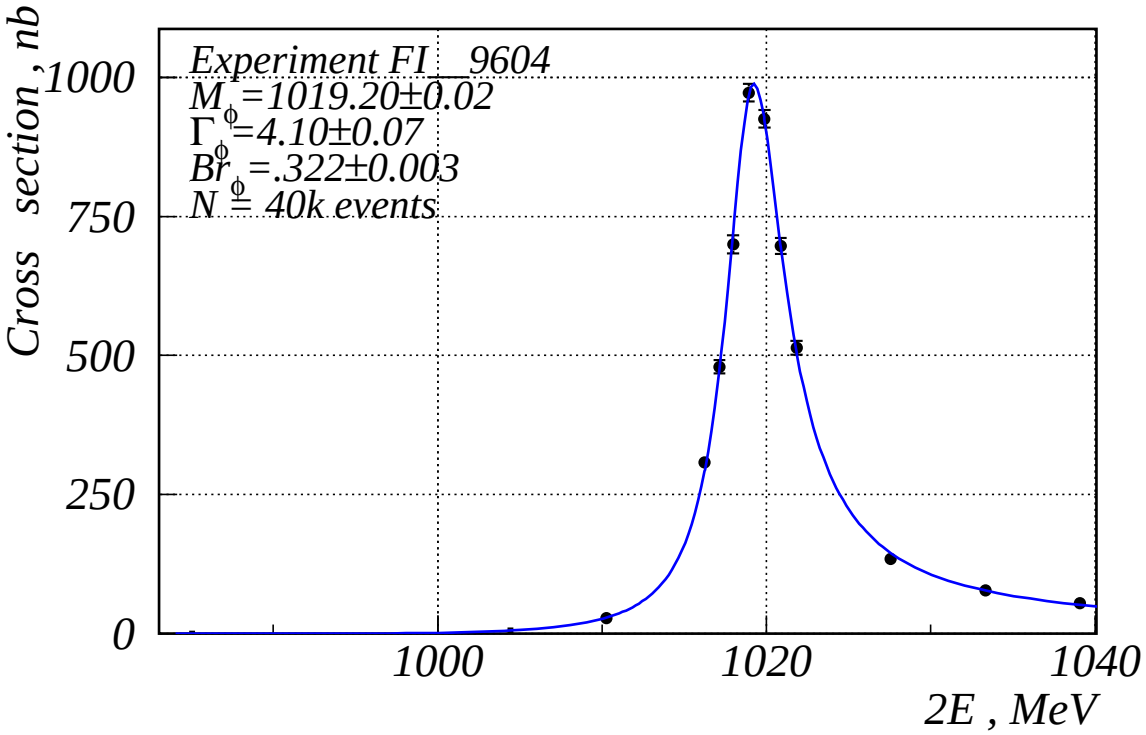

Figure 10: Cross section of the $e^+e^- \to \varphi \to K_S K_L$ process.

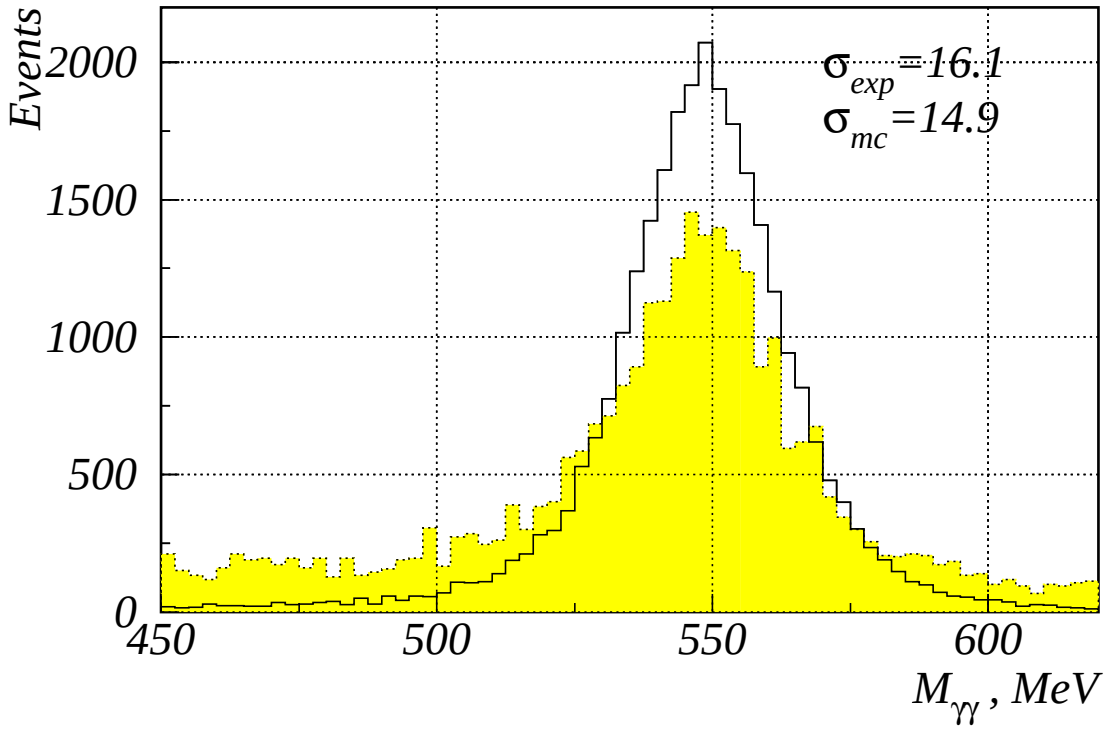

Figure 11: η- meson invariant mass in the $e^+e^- \to \varphi \to \eta\gamma$ process.

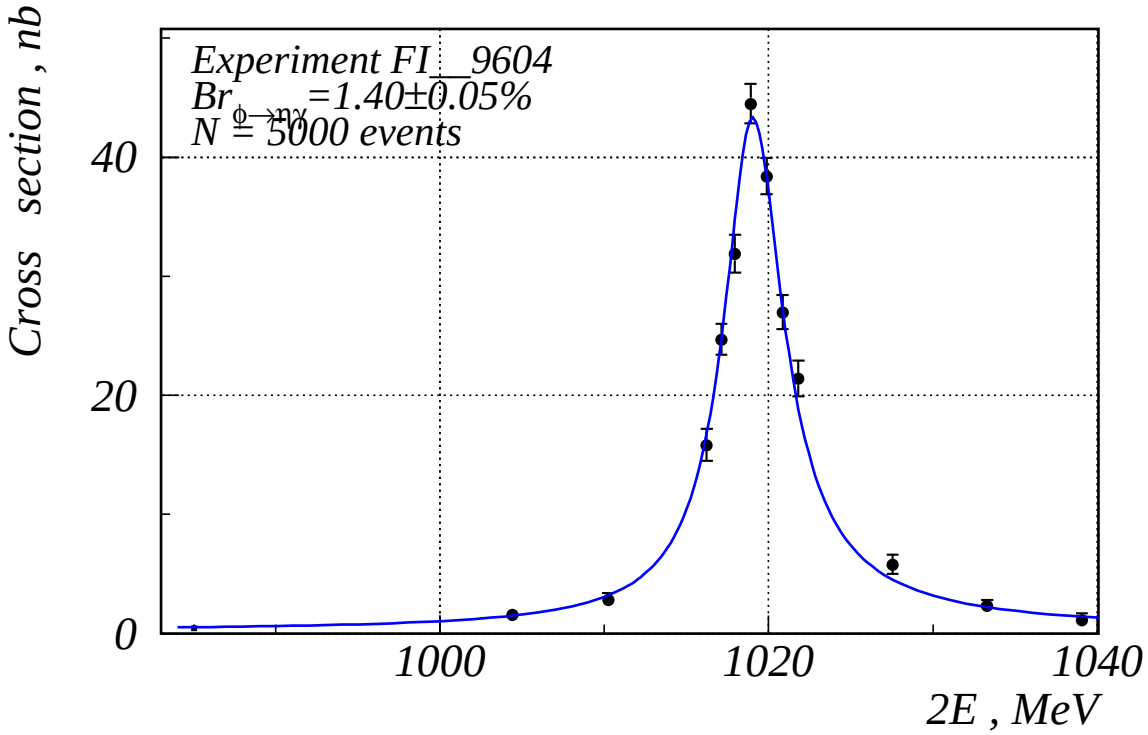

Figure 12: Cross section of the $e^+e^- \to \varphi \to \eta\gamma$ process.

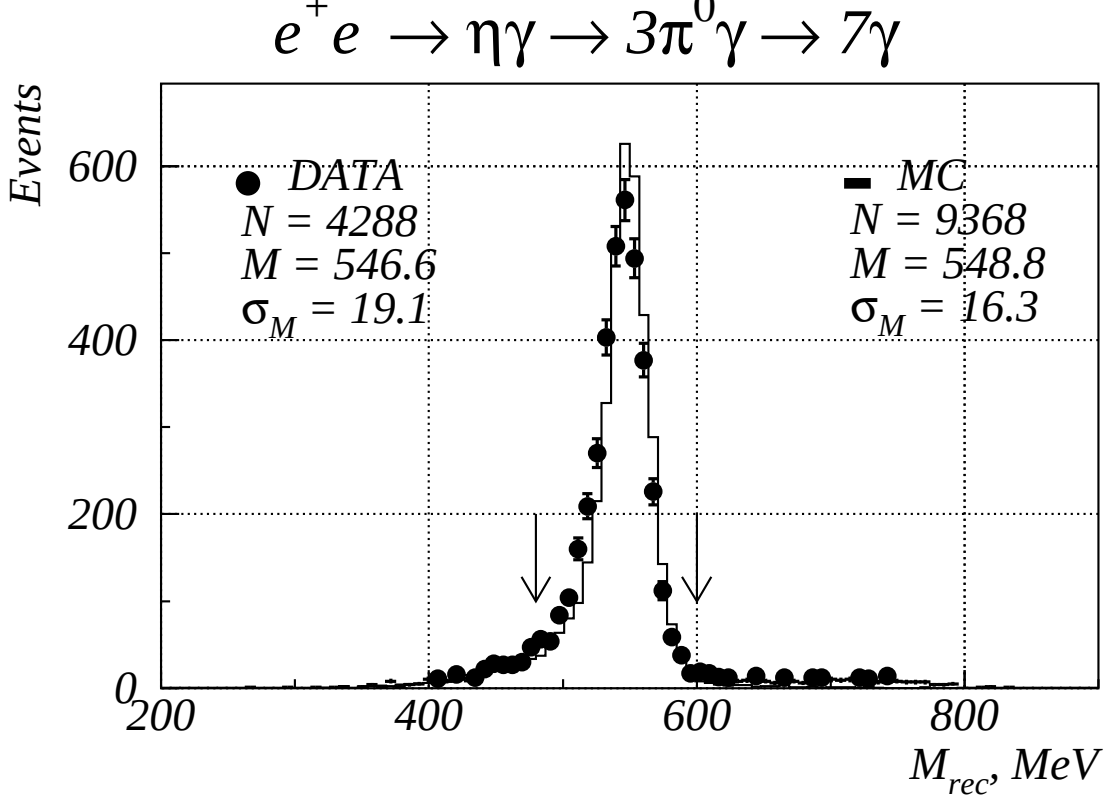

Figure 13: Recoil mass distribution for the most energetic photon.

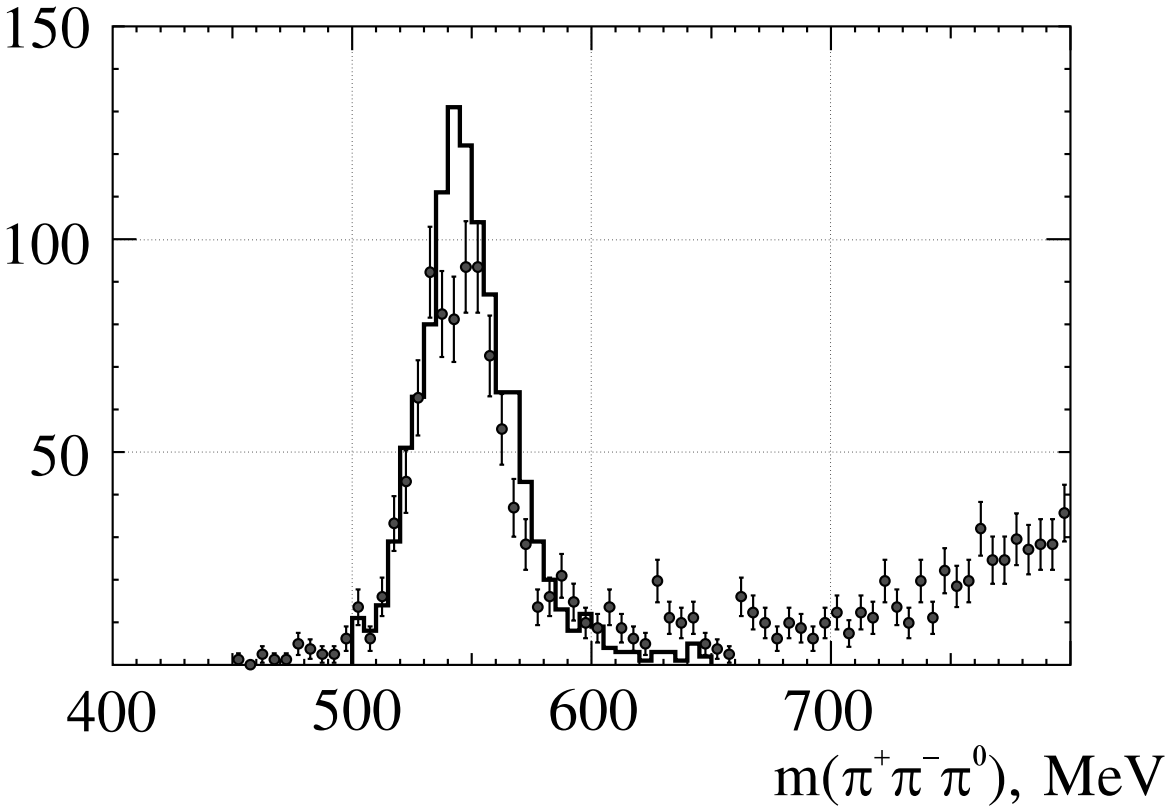

Figure 14: Distribution over the reconstructed mass of the η- meson; points with error bars — experiment, $\sigma_{exp} = 16.6\ MeV$; histogram — simulation, $\sigma_{sim} = 16.9\ MeV$.

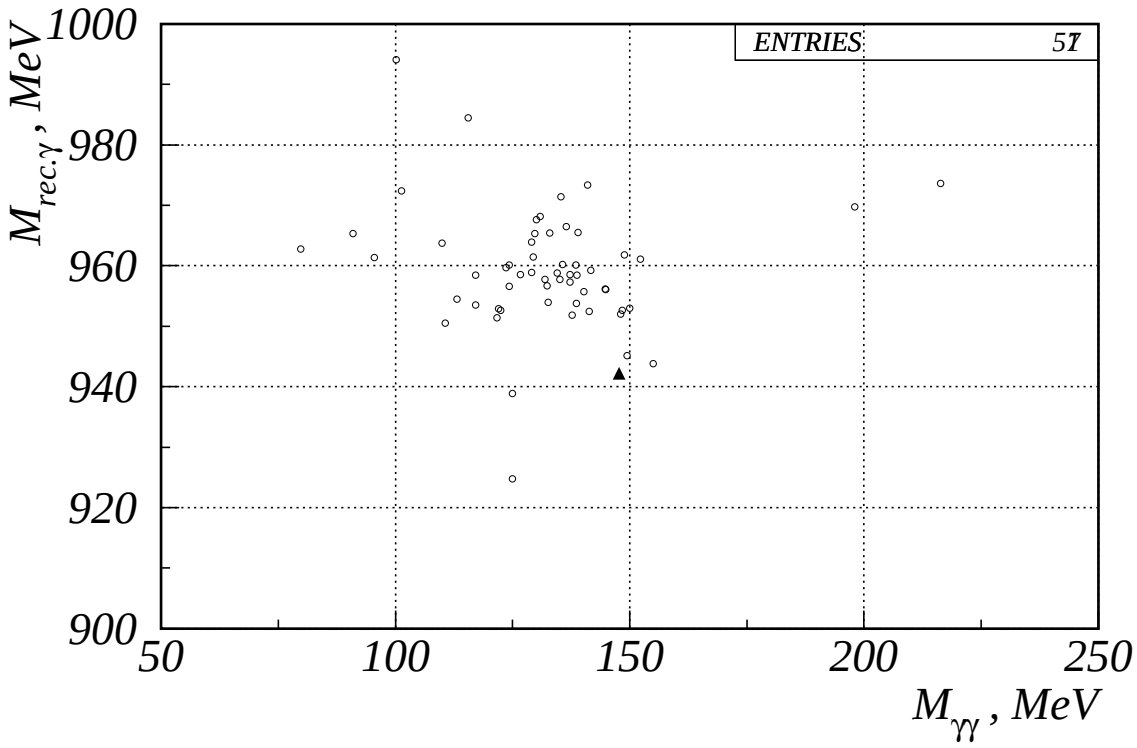

Figure 15: $m_{rec.\gamma}$ vs. $m_{\gamma\gamma}$ scatter plot for the $e^+e^- \to \varphi \to \eta'\gamma \to \pi^+\pi^-\pi^+\pi^-3\gamma$ decays. Circles — simulation, triangle — the event, satisfying selection criteria.

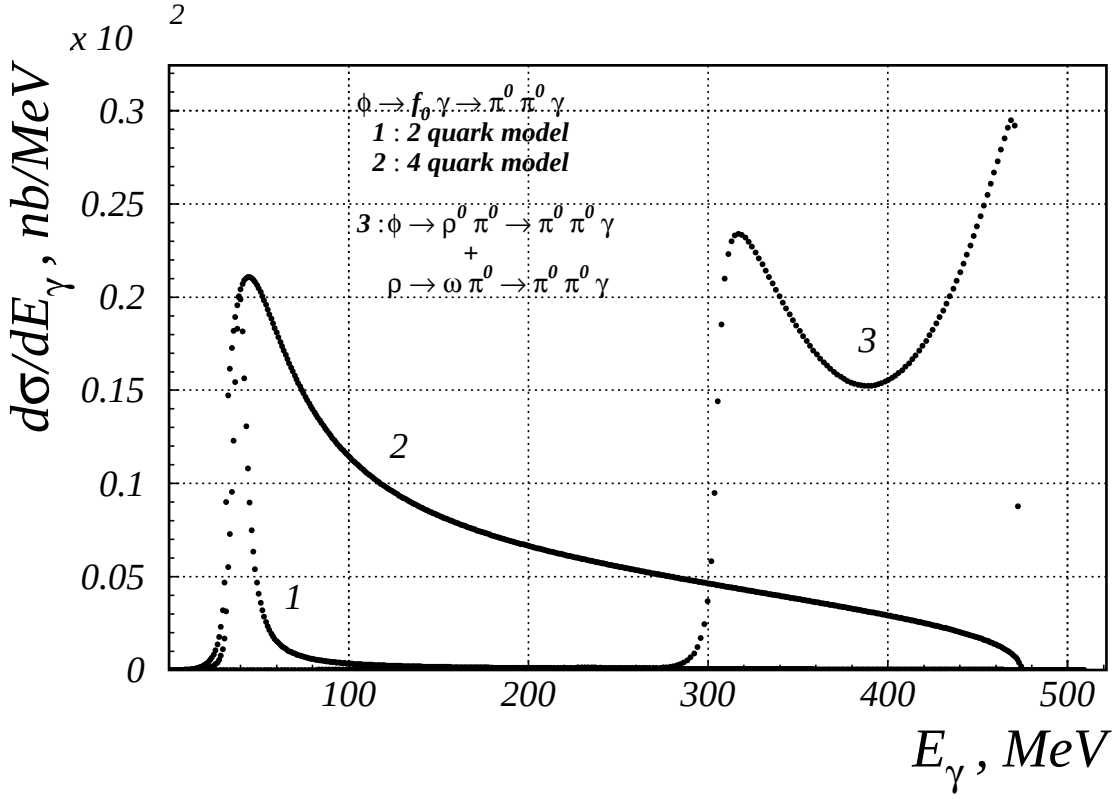

Figure 16: Recoil photon spectrum in the process $e^+e^- \to \pi^o\pi^o\gamma$.

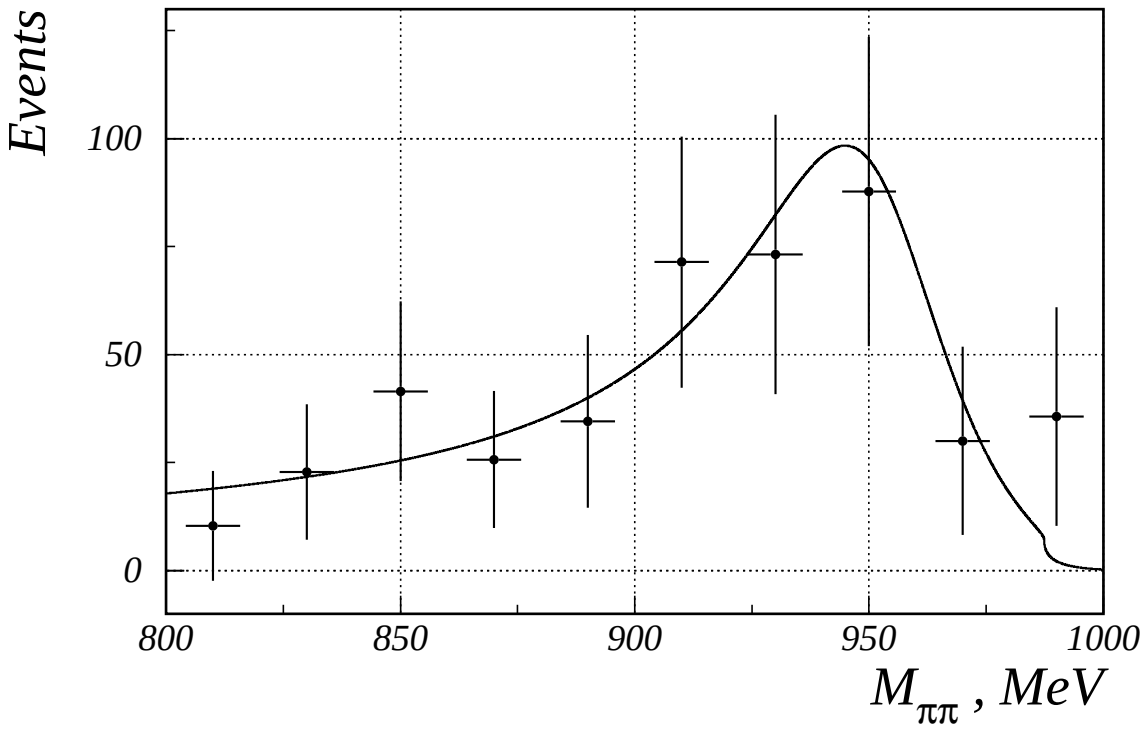

Figure 17: Distribution over invariant mass of the $\pi^o\pi^o$- system in the $e^+e^- \to \pi^o\pi^o\gamma$ process.

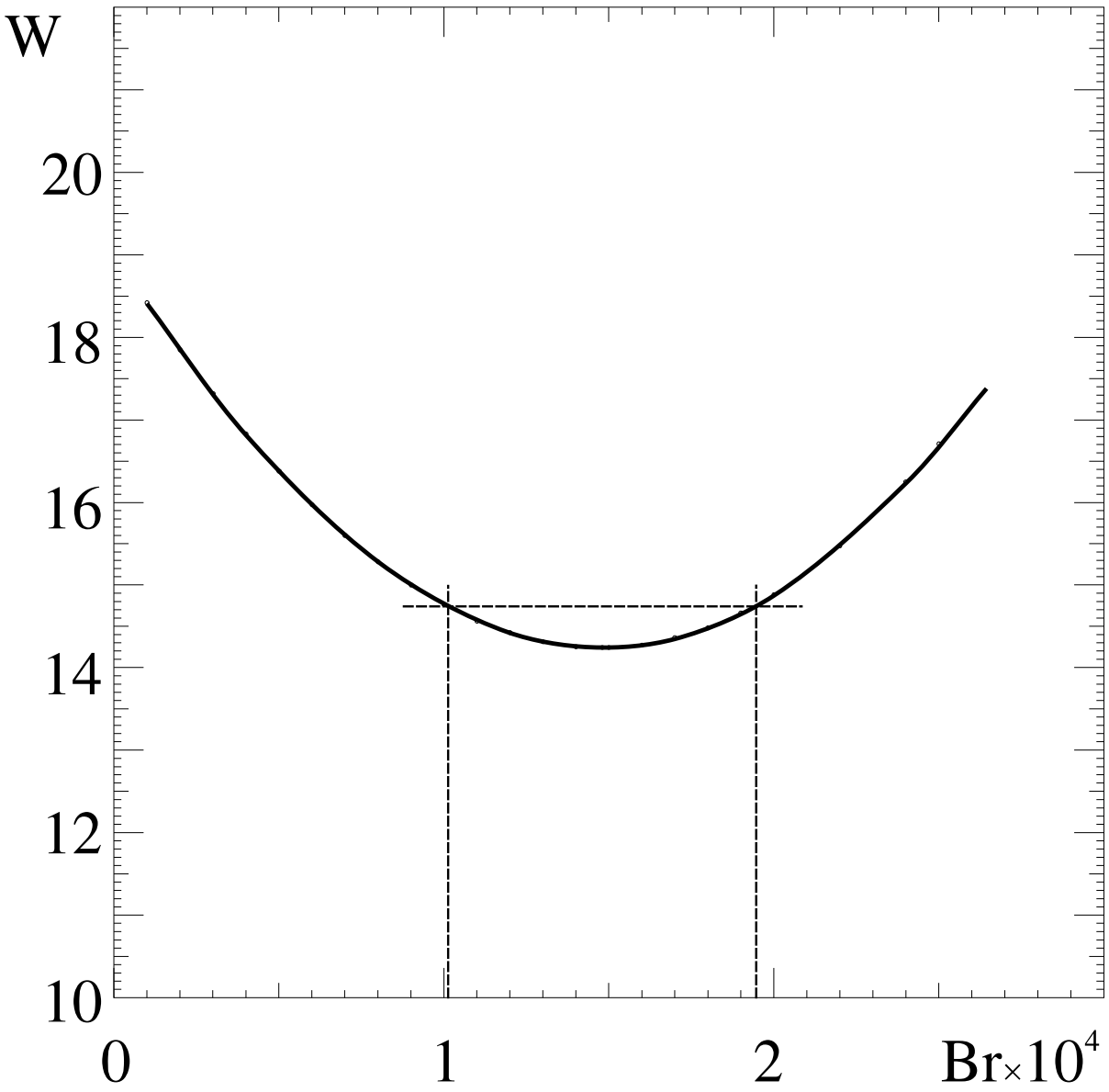

Figure 18: Dependence of maximum likelihood function on the $BR(\phi \to \eta\pi^0\gamma)$

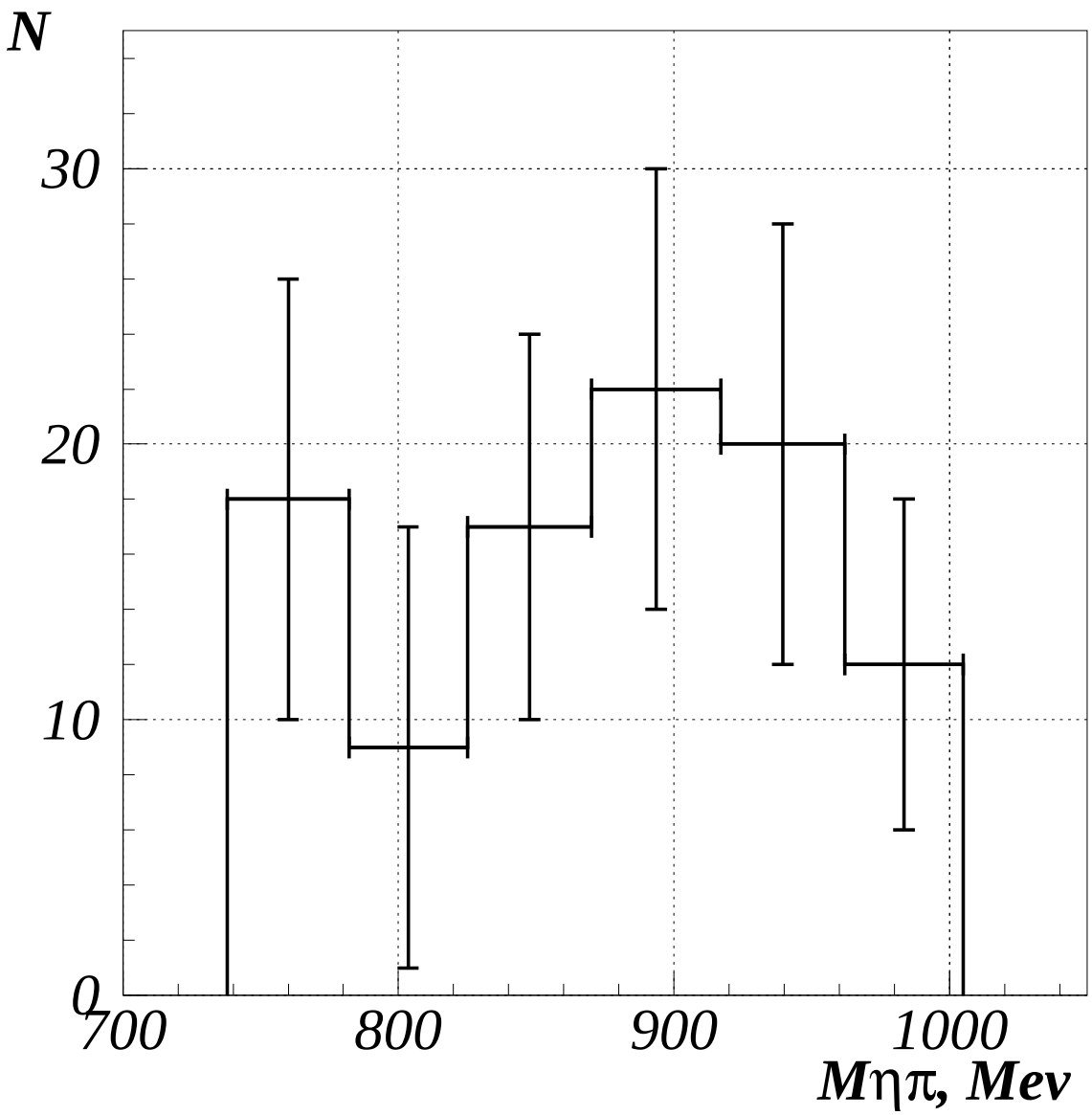

Figure 19: Measured mass spectrum of $\eta\pi^0$ system.

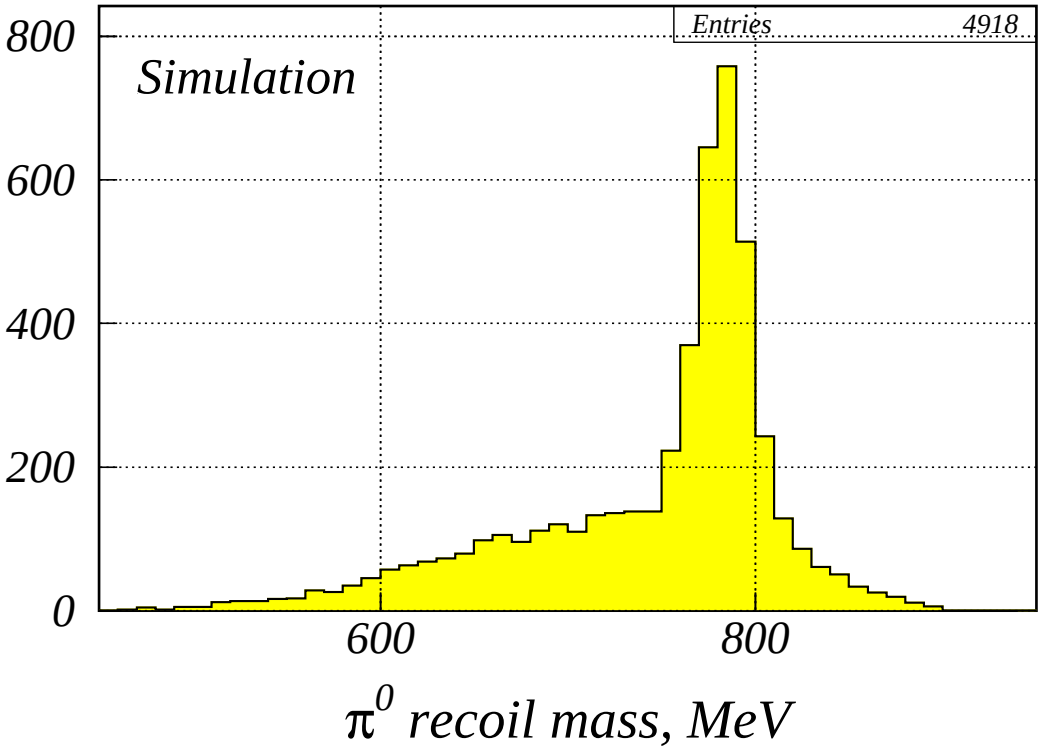

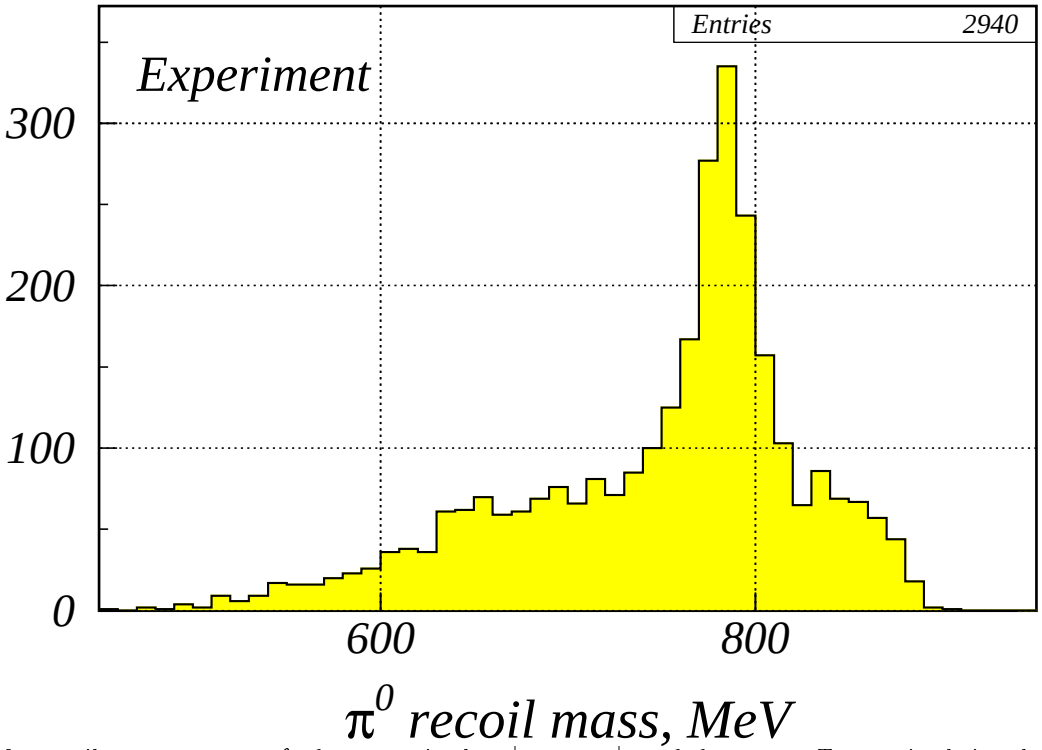

Figure 20: Recoil mass spectrum of π^o- mesons in the $e^+e^- \to \pi^+\pi^-\pi^o\pi^o$ process. Top — simulation; bottom — experiment.

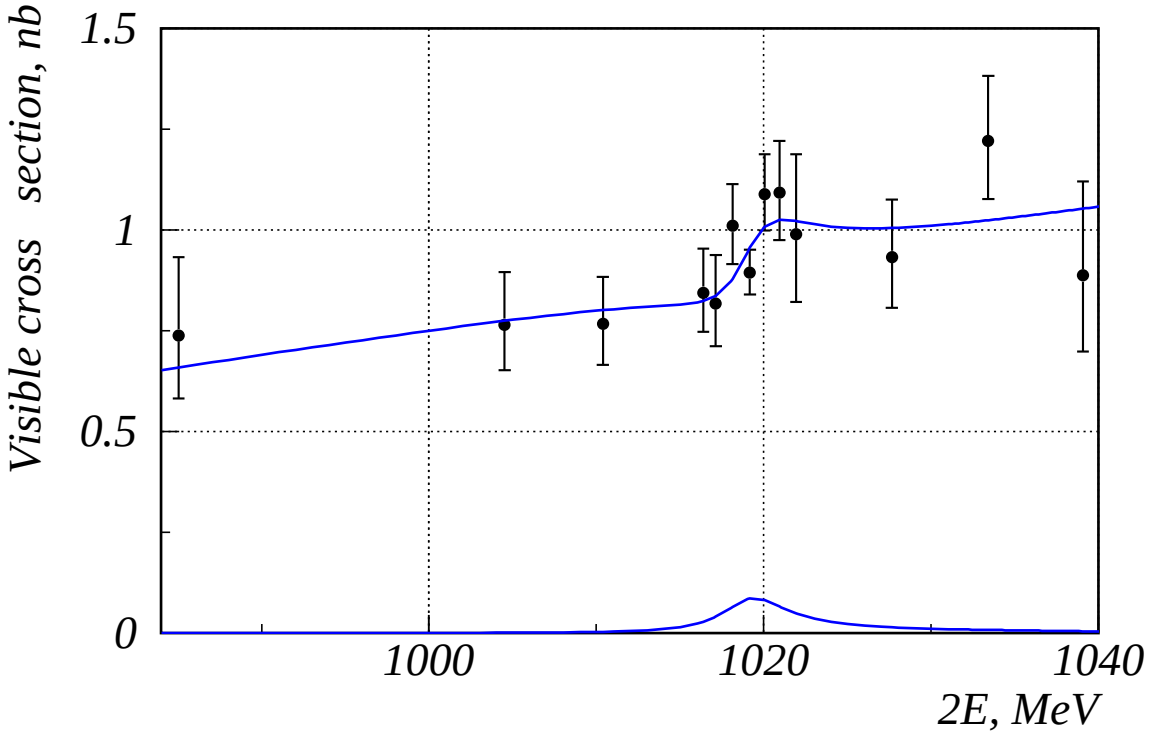

Figure 21: Detection cross section and fit parameters for the $e^+e^- \to \omega\pi^o \to \pi^+\pi^-\pi^o\pi^o$ process.

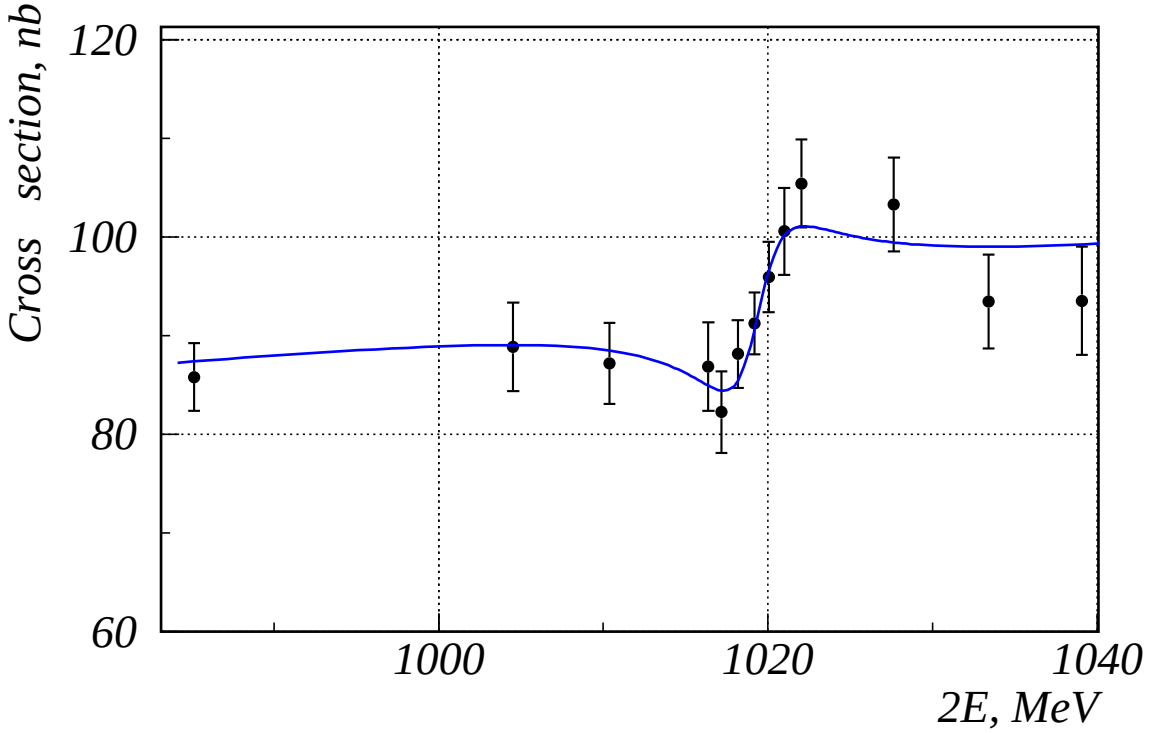

Figure 22: $e^+e^- \to \mu^+\mu^-$ cross section.

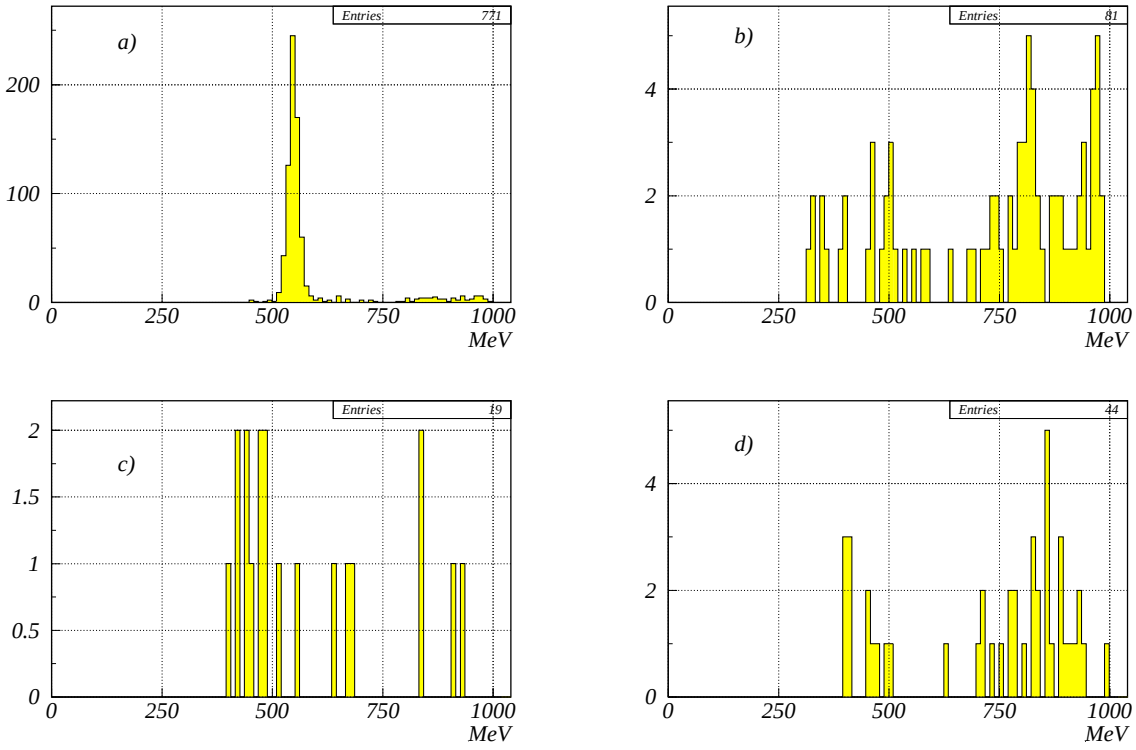

Figure 23: Photon recoil mass spectrum in the $e^+e^- \to \varphi \to \pi^o\pi^o\gamma$ process; a — $\eta \to 2\pi^o$ simulation; b — $\omega\pi^o$ ($\omega \to \pi^o\gamma$) simulation; c — $\eta \to 3\pi^o$ simulation; d — SND experiment.

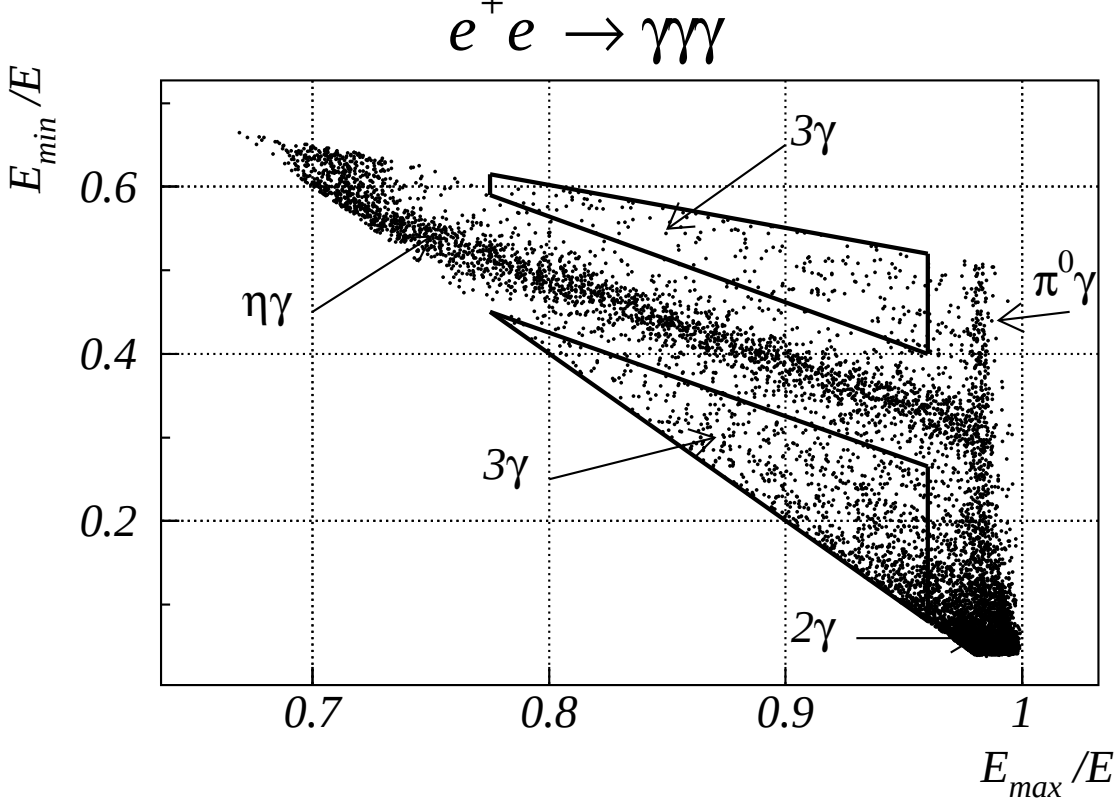

Figure 24: Dalitz plot for the events of the $e^+e^- \to 3\gamma$. process

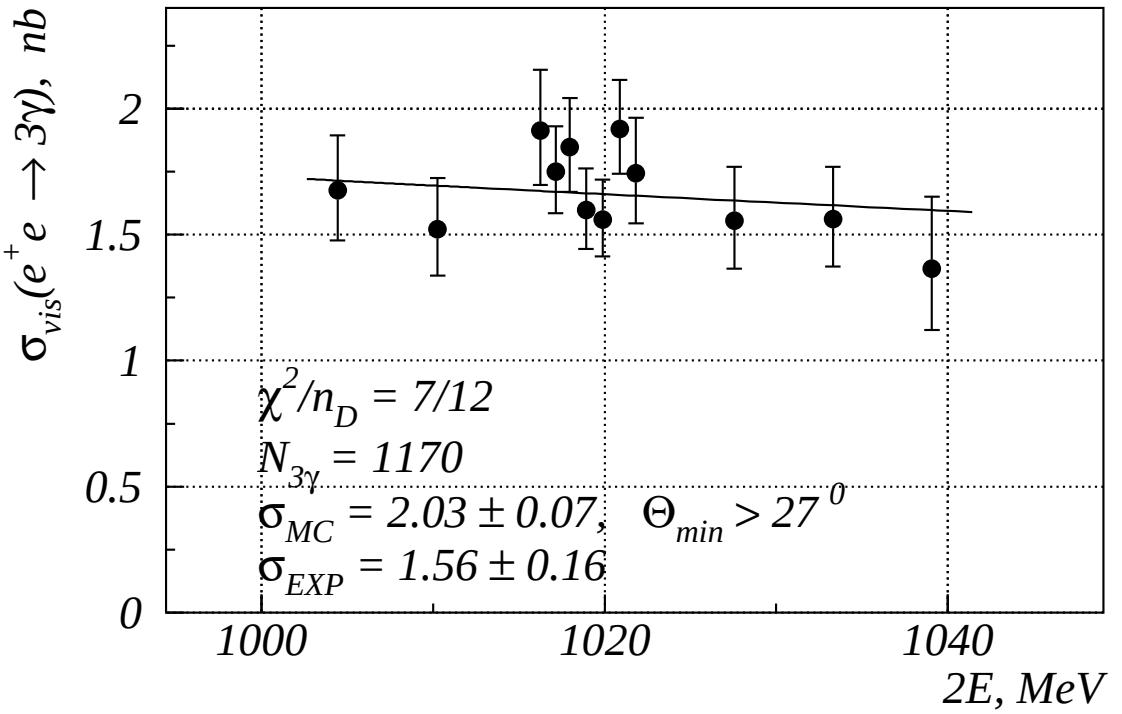

Figure 25: $e^+e^- \to 3\gamma$ detection cross section.

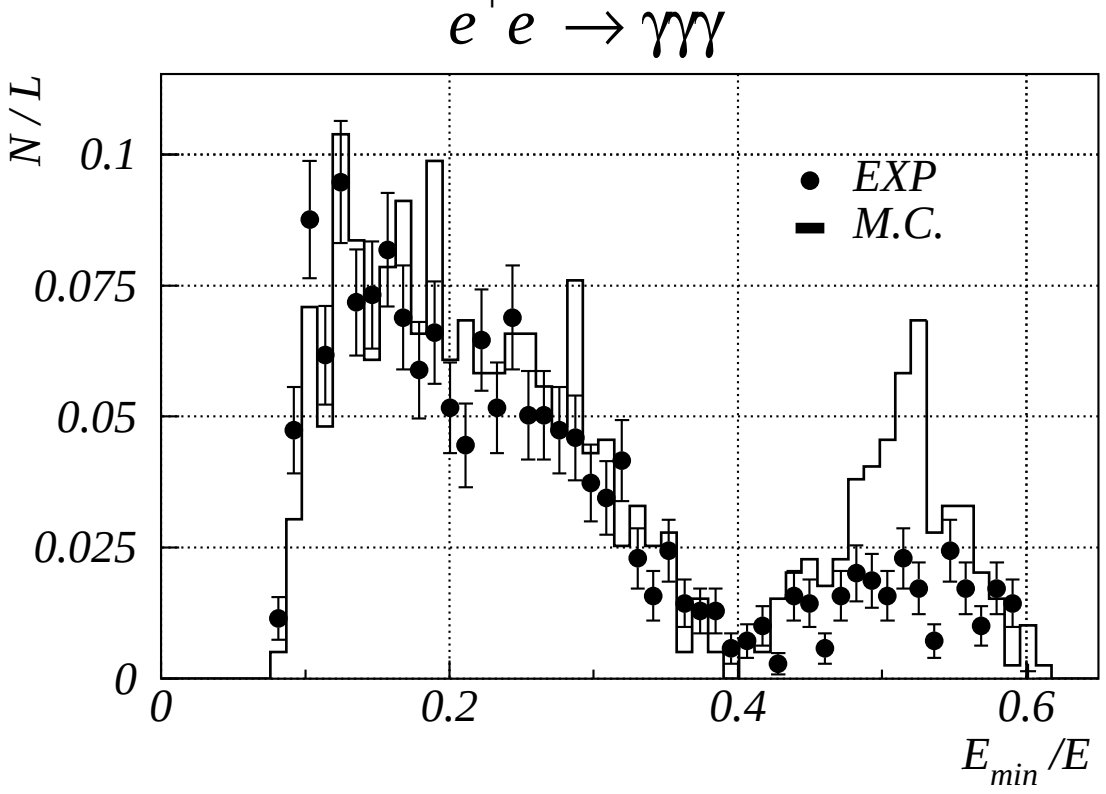

Figure 26: Lowest energy photon spectrum in $e^+e^- \to 3\gamma$ events.

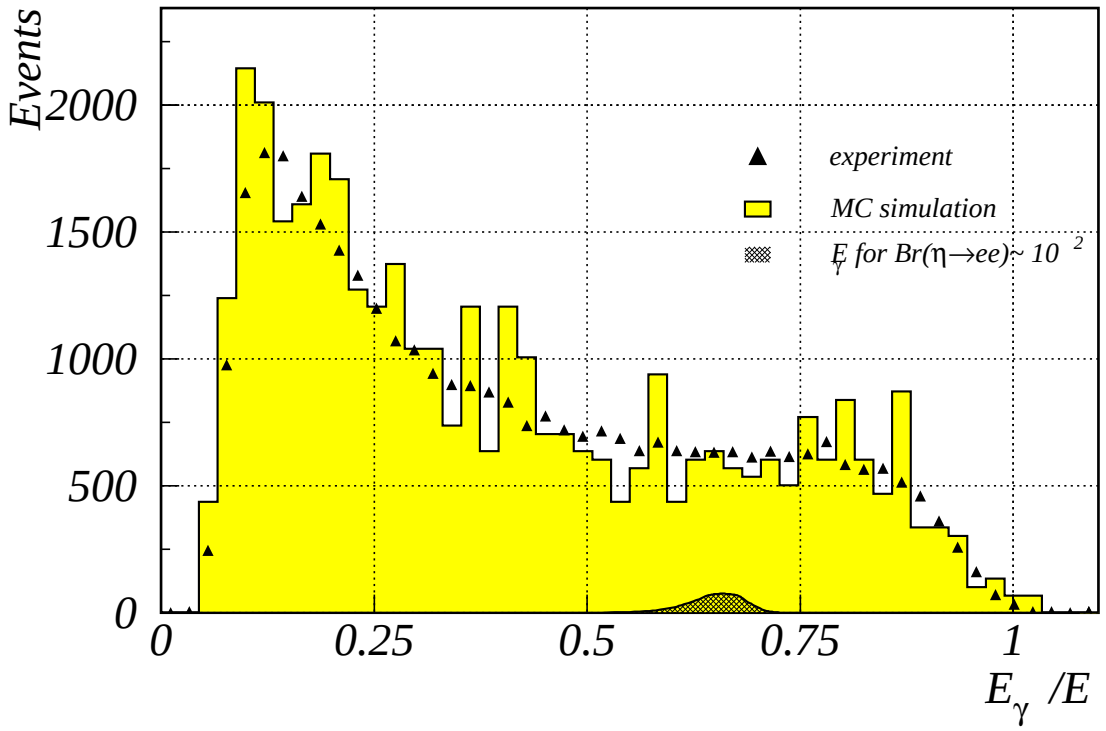

Figure 27: Photon spectrum in the $e^+e^- \to e^+e^-\gamma$ process. Peak at $E_\gamma = 0.7E$ comes from the possible $\eta \to e^+e^-\gamma$ decay with a branching ratio close to 1%.

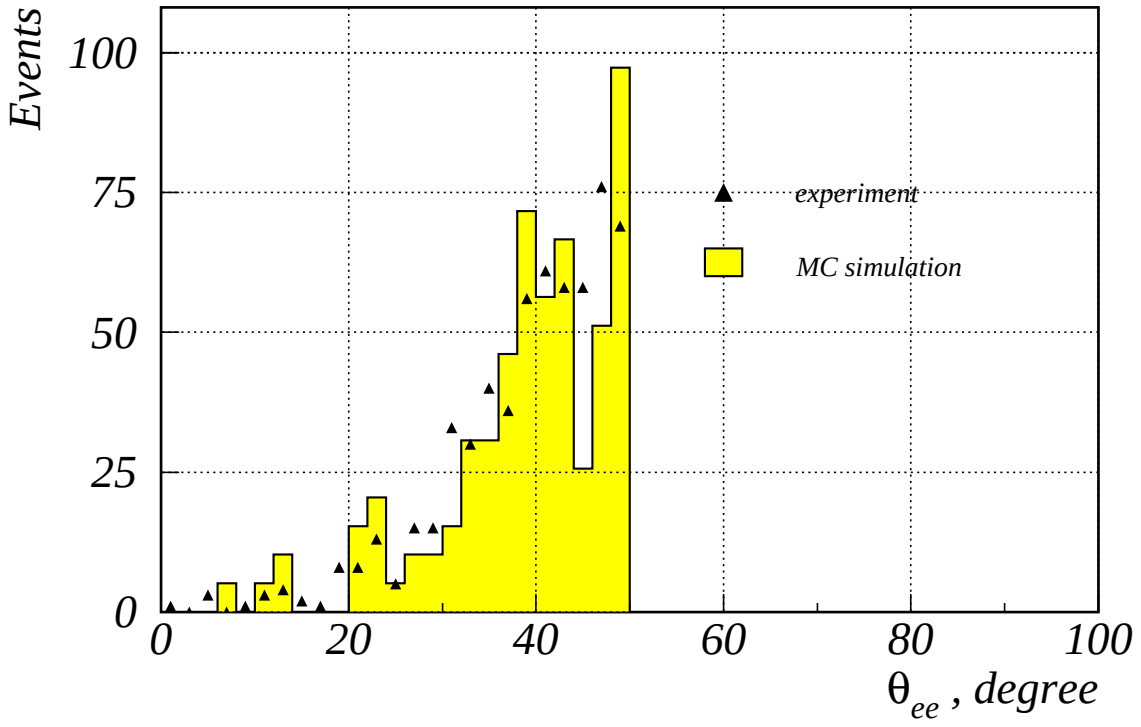

Figure 28: Distribution over the spatial angle between electrons in the $e^+e^- \to e^+e^-\gamma$ process.

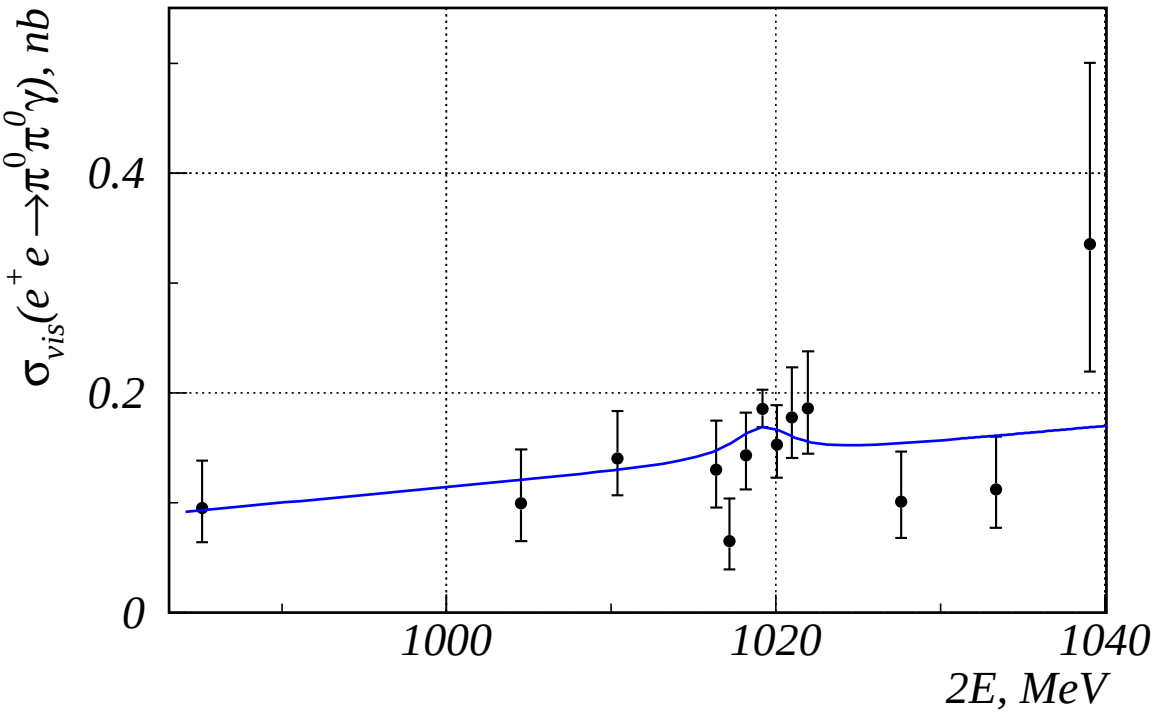

Figure 29: Cross section of the $e^+e^- \to \omega\pi^o$ process.

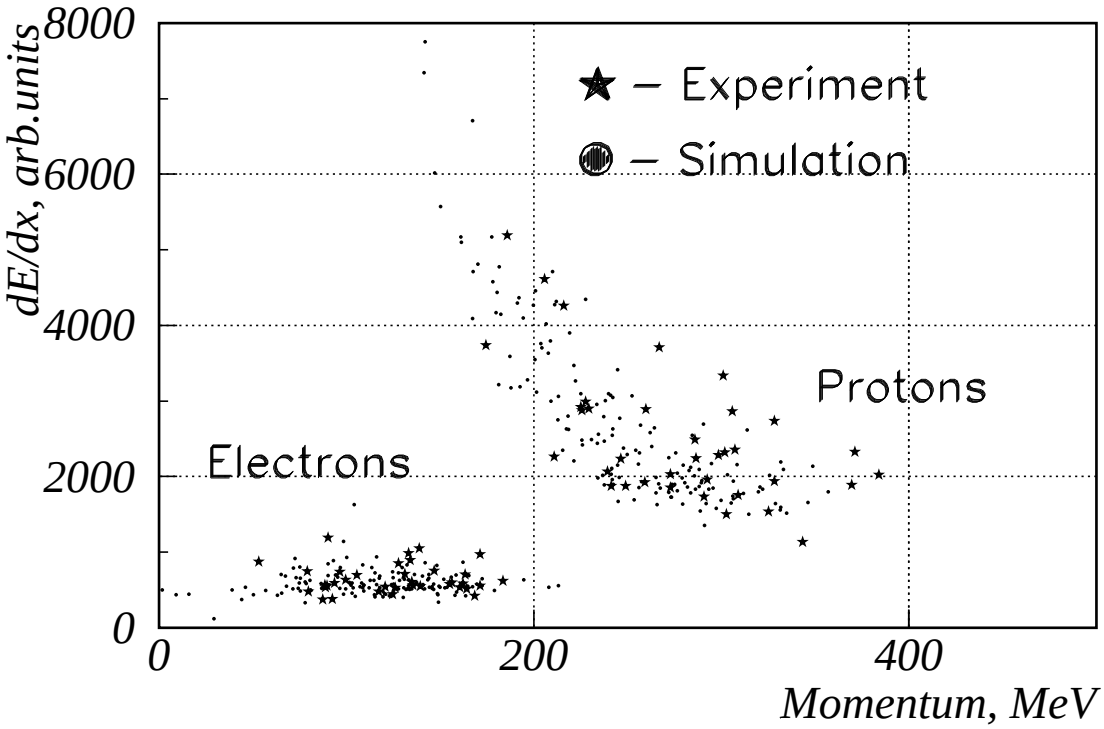

Figure 30: Dependence of dE/dx in the drift chamber on particle momentum. Experimental and simulated data for electrons and protons from the process $e^{\pm}p \to e^{\pm}\Delta^{+} \to e^{\pm}p\pi^{o}$ are shown.

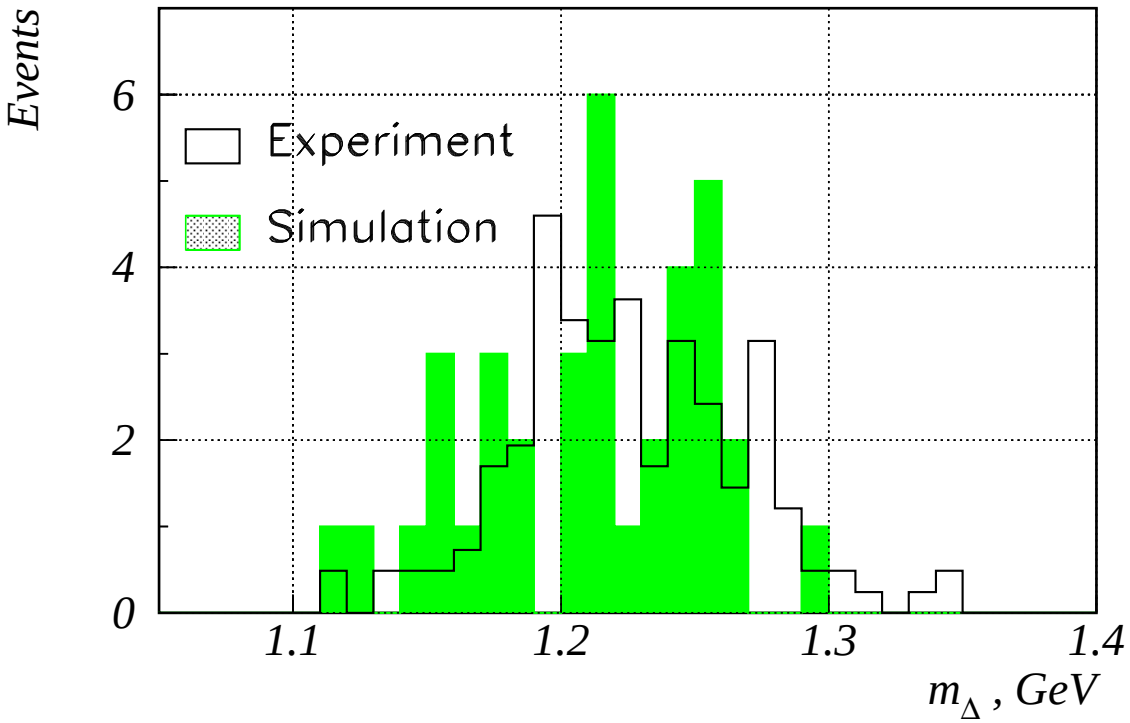

Figure 31: Distribution over invariant mass of proton and pion in the $e^{\pm}p \to e^{\pm}\Delta^{+} \to e^{\pm}p\pi^{o}$ process